Molecular Phylogenetics and Evolution 62 (2012) 130–145

Contents lists available at SciVerse ScienceDirect

Molecular Phylogenetics and Evolution

journal homepage: www.elsevier.com/locate/ympev

Phylogenetic inference rejects sporophyte based classification of the Funariaceae (Bryophyta): Rapid radiation suggests rampant homoplasy in sporophyte evolution

Yang Liu, Jessica M. Budke, Bernard Goffinet *

Department of Ecology and Evolutionary Biology, University of Connecticut, Storrs, CT 06269, USA

ARTICLE INFO

Article history:
Received 2 June 2011
Revised 9 September 2011
Accepted 17 September 2011
Available online 22 September 2011

Keywords:
Data partitioning
Monophyly test
Conflict visualization
Funariaceae
Physcomitrella

ABSTRACT

The moss family Funariaceae, which includes the model systems *Funaria hygrometrica* and *Physcomitrella patens*, comprises 15 genera, of which three accommodate approximately 95% of the 250–400 species. Generic concepts are drawn primarily from patterns in the diversity of morphological complexity of the sporophyte. Phylogenetic inferences from ten loci sampled across the three genomic compartments yield a hypothesis that is incompatible with the current circumscription of two of the speciose genera of the Funariaceae. The single clade, comprising exemplars of *Funaria* with a compound annulus, is congruent with the systematic concept proposed by Fife (1985). By contrast, *Entosthodon* and *Physcomitrium* are resolved as polyphyletic entities, and even the three species of *Physcomitrella* are confirmed to have diverged from distinct ancestors. Although the backbone relationships within the core clade of the Funariaceae remain unresolved, the polyphyly of these genera withstands alternative hypothesis testing. Consequently, the sporophytic characters that define these lineages are clearly homoplasious suggesting that selective pressures (or their relaxation) are in fact driving the diversification rather than the conservation of sporophytic architecture in the Funariaceae.

1. Introduction

The life cycle of mosses is characterized by a perennial vegetative body, the gametophyte, and a shorter-lived sporophyte, which remains permanently attached to the maternal plant. The sporophyte has often been considered less prone to change, because of its short lifespan and its critical function in spore dispersal (Allen et al., 1985; Edwards, 1984). Consequently, the features of the sporangium and in particular the architecture of the teeth lining the capsule mouth served as a basis for the suprageneric classification of mosses (Crosby, 1980; Goffinet et al., 2009; Vitt, 1984, 2000; Walther, 1983). However, recent phylogenetic reconstructions highlight that sporophytic traits are plagued by reduction (Bell and Hyvönen, 2010; Buck et al., 2000; Goffinet and Shaw, 2002; Hedderson et al., 1999), and that reduction can converge to similar morphologies in distantly related lineages (Goffinet et al., in press). Reversals to a plesiomorphic sporophyte (e.g., sessile or gymnostomous) is phylogenetically scattered among mosses and at least partially correlated with shifts to xeric habitats, where for example elaborate peristomes regulating spore dispersal may be superfluous (Vitt, 1981). Members of the moss family Funariaceae are mostly annuals, grow in ruderal habitats for one (rarely two) years, and are characterized by a rather uniform vegetative body and a broad diversity in sporophytic architecture, from sessile indehiscent capsules to sporangia elevated on a long seta with a complex annulus and double peristome. Here we test whether supraspecific taxa defined exclusively by a combination of sporophytic traits withstand a criterion of monophyly, and hence we provide a first assessment of the phylogenetic meaning of the generic concepts within the Funariaceae.

The architecture of the leafy gametophyte of the Funariaceae is rather highly conserved throughout the family: the stems are short, orthotropic, with a central strand of narrow putative water conducting or supporting cells; the branches are few at best, always sympodial; leaves are unistratose but costate, with rhombic, smooth and thin-walled cells that vary in size but are otherwise undifferentiated throughout the lamina; the plants are monoicous with perigonia developing at the apex of the stem and perichaetia terminating subapical innovations (Fife, 1985). The most deviating morphology is expressed by *Nanomitriella*, a monospecific genus endemic to Southeast Asia, and defined by linear strongly toothed leaves (Fife, 1985). Only the calyptra, a hood derived from the maternal gametophyte that protects the developing sporophyte, varies across the family from cucullate to mitrate and from large

* Corresponding author. Fax: +1 860 486 6364.
E-mail address: bernard.goffinet@uconn.edu (B. Goffinet).

1055-7903/$ - see front matter © 2011 Elsevier Inc. All rights reserved.
doi:10.1016/j.ympev.2011.09.010

to barely covering the apex of the mature capsule. The sole gametophytic character that is unique and expressed in all Funariaceae is the pyriform to globose terminal cell of the paraphyses in the perigonia (Fife, 1985).

In contrast to the vegetative body, the sporophyte exhibits a conspicuous diversity in complexity: the seta is elongated or virtually lacking; the capsule is curved or erect with or without a well differentiated sterile neck; dehiscence follows a subapical line or is irregular; the annulus in operculate taxa is composed of two rings or one, is revoluble or not; the peristome comprises two or one rings or is lacking. Although only a minority of Funariaceae bear a well-developed peristome, its architecture is unique among mosses: the peristome is diplolepideous but the teeth (or segments) of the endostome lay opposite the exostome teeth, the ontogeny of the inner peristomial layer involves symmetric divisions that demarcate two consecutive segments (Goffinet et al., 1999; Schwartz, 1994; Shaw et al., 1989). In the absence of a peristome, the shape of the stomata guard cell may help diagnose the Funariaceae: the stoma is defined by a single cell, which appears doughnut-shaped, a trait, however, also seen in some Polytrichaceae (Paton and Pearce, 1957). Consequently, the Funariaceae can only be unambiguously diagnosed by a single morphological character, the shape of their paraphyses.

The Funariaceae comprise approximately 250–400 species accommodated in 15 genera, of which *Entosthodon*, *Funaria* and *Physcomitrium* hold all but 16 species (Crosby et al., 1999; Fife, 1985). Ten genera are monospecific and two comprise three species (i.e., *Physcomitrella* and *Goniomitrium*). Most of the genera are defined by a combination of sporophytic character states, and hence individual traits may occur in more than one genus. While the circumscription of *Physcomitrium*, which is defined by erect capsules lacking a peristome, and a mitrate calyptra, has been widely accepted, the segregation of *Entosthodon* from *Funaria* has been repeatedly challenged. A broad concept of *Funaria* was adopted among others by Lindberg (1870, 1879) Brotherus (1903, 1924–1925), Smith (1978) and Crum and Anderson (1981), whereas Mueller (1849–1851), and Vitt (1982, 1984) recognized both genera. Fife (1985) proposed the first revision of the generic circumscriptions within the Funariaceae based on a global perspective of the morphological diversity, and concluded that *Funaria* should be distinguished from *Entosthodon* based on its compound annulus, a complex ring of cells accounting for the release of the operculum from the sporangium. Although *Entosthodon* is now widely recognized as a distinct genus, its diagnosis varies. Indeed, the genus is most often defined by the architecture of its peristome (reduced versus double in *Funaria*; e.g., Frahm, 1995; McIntosh, 2007; Miller and Miller, 2007; Smith, 2004), resulting in generic circumscriptions that deviate from the ones proposed by Fife (1985). Only Brugués and Ruiz (2010) seem to follow Fife's generic concept. The status of most monospecific genera has remained unchallenged except for *Aphanorrhegma*, which Corley et al. (1981) broadened to include *Physcomitrella*. This concept was supported by Ochyra (1983) who argued that the lack of a differentiated equatorial line of sporangial dehiscence in *Physcomitrella* did not justify the generic segregation.

The Funariaceae include *Funaria hygrometrica* Hedw. and *Physcomitrella patens* (Hedw.) Bruch and Schimp., which served and continue to serve as model systems for studies in hybridization (Bauer and Brosig, 1959; Bryan, 1957; von Wettstein, 1924), in physiology, developmental biology, genetics and more recently in functional genomics (Cove, 2005; Schaefer and Zrÿd, 2001). In fact *P. patens* is the first non-flowering land plant to have its entire three genomes sequenced (Rensing et al., 2008; Sugiura et al., 2003; Terasawa et al., 2007) and serves as a critical taxon for the study of gene and genome evolution in land plants (Knight et al., 2009). Despite this critical role in furthering our understanding of bryophyte and land plant biology, the phylogeny of the Funariaceae remains widely unresolved. The family is closely related to the Encalyptales and Disceliaceae, a common ancestry defined by a unique inversion of 71 kb in the chloroplast genome (Goffinet et al., 2007). The Gigaspermaceae and Ephemeraceae have been excluded from the Funariales based on phylogenetic evidence (Goffinet et al., 2007, in press; Werner et al., 2007). The core of the family is likely monophyletic, and the genera are distributed between two sister lineages, the Pyramiduloideae (*Goniomitrium* and *Pyramidula*) and Funarioideae (remaining genera; Werner et al., 2007). The relationships within the Funarioideae have not been critically reconstructed as previous inferences were drawn from variation in few genetic loci sampled from a small set of exemplars (e.g., Goffinet and Cox, 2000; Werner et al., 2007). Most recently, however, McDaniel et al. (2010) and Hooper et al. (2010) demonstrated that *Physcomitrella* is polyphyletic with species arising independently within *Physcomitrium*.

The current study focuses on reconstructing the generic relationships within the Funarioideae based on a broader sampling of loci and generic exemplars, to test for the monophyly of speciose genera traditionally defined by a combination of sporophytic traits (i.e., *Entosthodon*, *Funaria* and *Physcomitrium*).

2. Materials and methods

We have reconstructed the phylogenetic relationships among exemplars of the Funariidae using species of the Timmiidae as the outgroup. We targeted twelve loci, tested the effect of partitioning the data on the topology and the robustness of the branches, and assessed whether monophyly of genera as currently defined is supported by the data.

2.1. Taxon and gene sampling

To reconstruct a backbone phylogeny of the Funariaceae we sampled 30 exemplars representing 26 species and nine genera of this family and rooted it with taxa of the Encalyptaceae, Disceliaceae, Gigaspermaceae using Timmiaceae as the ultimate outgroup (Goffinet and Cox, 2000; Goffinet et al., 2001). Voucher information and GenBank accession numbers of sequences are provided in Table 1.

We targeted 12 DNA loci, three nuclear (nu): the adenosine kinase gene (*adk*, spanning exon 8–11), heme oxygenase gene (*ho*, spanning exon 2–4) and the ribosomal internal transcribed spacer (ITS); five chloroplast (cp): the noncoding spacer between the *atp*B and *rbc*L genes (*atp*B–*rbc*L), *pet*D–*pet*N noncoding region (*pet*D–N), *psb*A–*trn*H noncoding region (*psb*A–*trn*H), ribosomal small protein 4 gene (*rps*4) and *trn*L (UAA)-*trn*F (GAA) region (*trn*L–F); four mitochondrial (mt): *atp*1–*trn*W noncoding region (*atp*1–*trn*W), nad2–*trn*G (*nad*2–*trn*G) noncoding region, the ribosomal protein L2 (*rpl*2) and *rps*7–*atp*6 noncoding region (*rps*7–*atp*6). As to these fragments, ITS and four of the five chloroplast loci have been widely used in bryophyte phylogenetic studies (Stech and Quandt, 2010). The cp *pet*D–N locus had previously been sequenced, but not used for phylogenetic analyses by Goffinet et al. (2007). The four mitochondrial loci are targeted for the first time for bryophytes.

2.2. DNA extraction, amplification and sequencing

DNA extraction, PCR amplification and sequencing followed protocols as described in Goffinet et al. (2007). For some accessions we cloned the amplicons of cp *pet*D–N, mt *rps*7–*atp*6 and nu ITS into the *Escherichia coli* vector using the TOPO TA cloning kit (Invitrogen, California, USA). Positive *E. coli* colonies were picked

Table 1
Voucher information and GenBank accession numbers for taxa sequenced in this study. Except for those in bold, sequences are newly generated.

Taxon	Collection number	Locality	Herbarium	Nuclear	Chloroplast					Mitochondrial			
				ITS	*atp*B–*rbc*L	*trn*L–F	*pet*N–*pet*D	*psb*A–*trn*H	*rps*4	*rpl*2	*atp*1–*trn*W	*rps*7–*atp*6	*nad*2–*trn*G
Aphanorrhegma serratum 1	BG-NC	USA	DUKE	JN089155	JN089196	JN088933	JN089085	JN089041	JN088967	JN088998	JN089281	JN089239	JN089111
Aphanorrhegma serratum 2	Buck 49500	USA	NYBG	JN089156	JN089197	JN088934	JN089086	JN089042	JN088968	JN088999	JN089282	JN089240	JN089112
Bryobartramia novae-valesiae	Magill and Schelpe 3218a	South Africa	DUKE	JN089157	JN089198	JN088935	**EF173140**	JN089043	**AY908160**	JN089000	JN089283	JN089241	JN089113
Bryobeckettia bartlettii	Beveridge 564868	New Zealand	CHR	JN089158	JN089199	JN088936	JN089087	JN089044	JN088969	JN089001	JN089284	JN089242	JN089114
Bryobrittonia longipes	Ignatov 1997	Russia	NYBG	JN089159	JN089200	**DQ397197**	JN089088	JN089045	JN088970	JN089002	JN089285	JN089243	JN089115
Chamaebryum pottioides	Koekemoer 2490	South Africa	CONN	JN089160	JN089201	**AF229908**	–	JN089046	**AF223051**	JN089003	JN089286	JN089244	JN089116
Costesia spongiosa	Larrain and Zegers 27172	Chile	CONN	–	JN089202	JN088937	–	JN089047	JN088971	JN089004	JN089287	JN089245	JN089117
Discelium nudum	Smith 47503	USA	NYS	JN089161	JN089203	**AF229920**	**EF173139**	JN089048	**AF223063**	JN089005	JN089288	JN089246	JN089118
Encalypta armata	Goffinet 5613	Chile	CONN	JN089162	JN089204	JN088938	**EF173150**	JN089049	**AF223039**	JN089006	JN089289	JN089247	JN089119
Encalypta ciliata	Schofield 98872	USA	DUKE	JN089163	JN089205	**AF229897**	JN089089	JN089050	**AY908161**	JN089007	JN089290	JN089248	JN089120
Entosthodon apophysatus	Bellolio 31919	Chile	CONN	JN089164	JN089206	JN088939	JN089090	JN089051	JN088972	JN089008	JN089291	JN089249	JN089121
Entosthodon bonplandii	Goffinet 6326	Mexico	CONN	JN089165	JN089207	AF229899	**EF173153**	JN089052	**AF223042**	JN089009	JN089292	JN089250	JN089122
Entosthodon drummondii	Shaw s.n.	-	DUKE	JN089166	JN089208	JN088940	JN089091	JN089053	**AF306961**	JN089010	JN089293	JN089251	JN089123
Entosthodon fascicularis	Frahm 20.4.94	Germany	CONN	JN089167	JN089209	JN088941	JN089092	JN089054	JN088973	JN089011	JN089294	JN089252	JN089124
Entosthodon laevis	Goffinet 5601	Chile	CONN	JN089168	JN089210	**AF229900**	**EF173151**	JN089055	**AY908156**	JN089012	JN089295	JN089253	JN089125
Entosthodon laxus	Fife 12133	New Zealand	CHR	–	JN089211	JN088942	JN089093	JN089056	JN088974	JN089013	JN089296	JN089254	JN089126
Entosthodon muhlenbergii	Lüth 5431	Greece	Lüth[a]	JN089169	JN089212	JN088943	JN089094	JN089057	JN088975	JN089014	JN089297	JN089255	JN089127
Entosthodon obtusus	Holyoak 04-87	Ireland	CONN	JN089170	JN089213	JN088944	JN089095	JN089058	JN088976	JN089015	JN089298	JN089256	JN089128
Entosthodon pulchellus	Lüth 5365	Greece	Lüth[a]	JN089171	JN089214	JN088945	JN089096	JN089059	JN088977	JN089016	JN089299	JN089257	JN089129
Entosthodon serratus	Frank and Robert 13109	USA	WIS	JN089172	JN089215	JN088946	EF173156	JN089060	JN088978	JN089017	JN089300	JN089258	JN089130
Funaria flavicans	Goffinet 9345	USA	CONN	JN089173	JN089216	JN088947	JN089097	JN089061	JN088979	JN089018	JN089301	JN089259	JN089131
Funaria hygrometrica	Goffinet 5576	Chile	CONN	JN089174	**DQ397164**	JN088948	EF173160	JN089062	JN088980	**JN089019**	**JN089302**	**JN089260**	**JN089132**
Funaria microstoma	Beever 95-09	Australia	CONN	JN089175	JN089217	JN088949	JN089098	JN089063	JN088981	JN089020	JN089303	JN089261	JN089133
Funariella curviseta	Ros and Werner 26-3-2006	Spain	MUB	JN089176	JN089218	JN088950	JN089099	JN089064	JN088982	JN089021	JN089304	JN089262	JN089134
Gigaspermum mouretii	Garcia-Zamora 7891	Spain	CONN	JN089177	JN089219	JN088951	–	JN089065	JN088983	JN089022	JN089305	JN089263	JN089135
Gigaspermum repens	Schofield 90527	Australia	DUKE	JN089178	JN089220	JN088952	–	JN089066	JN088984	JN089023	JN089306	JN089264	JN089136
Goniomitrium acuminatum	Curnow and Lepp 6532	Australia	CONN	JN089179	JN089221	**DQ337181**	JN089100	JN089067	**DQ337185**	JN089024	JN089307	JN089265	JN089137
Goniomitrium seroi	Puche 18068	Spain	CONN	JN089180	JN089222	**DQ337178**	JN089101	JN089068	**DQ337186**	JN089025	JN089308	JN089266	JN089138
Lorentziella imbricata 1	Rushing December 2009	USA	CONN	JN089181	JN089223	JN088953	–	JN089069	JN088985	JN089026	JN089309	JN089267	JN089139
Lorentziella imbricata 2	Schinini 24785	Argentina	NY	JN089182	JN089224	JN088954	–	JN089070	JN088986	JN089027	JN089310	JN089268	JN089140
Oedipodiella australis	Thouvenot 27-November-05	France	CONN	JN089183	JN089225	JN088955	–	JN089071	JN088987	JN089028	JN089311	JN089269	JN089141
Physcomitrella magdalenae	Buchbender RWA-VB-0107	Rwanda	IMSC[b]	JN089326	JN089226	JN088956	JN089102	JN089072	JN088988	JN089029	JN089312	–	JN089142
Physcomitrella patens 1	Christy 9013	USA	DUKE	JN089184	JN089227	JN088957	JN089103	JN089073	JN088989	JN089030	JN089313	JN089270	JN089143
Physcomitrella patens 2	Withehouse 1962	UK	IMSC[b]	JN089185	JN089228	JN088958	JN089104	JN089074	**AP005672**	JN089031	JN089314	JN089271	JN089144
Physcomitrella readeri	Entrer 17545	USA	MO	JN089186	JN089229	JN088959	JN089105	JN089075	JN088990	JN089032	JN089315	JN089272	JN089145
Physcomitrium immersum 1	Christy 8505-1	USA	DUKE	JN089187	JN089230	JN088960	JN089106	JN089076	JN088991	JN089033	JN089316	JN089273	JN089146
Physcomitrium immersum 2	Blanka Shaw 4827	USA	DUKE	JN089188	JN089231	JN088961	JN089107	JN089077	JN088992	–	JN089317	–	JN089147
Physcomitrium lorentzii	Goffinet 5348	Chile	CONN	JN089189	JN089232	**AF229903**	JN089108	JN089078	**AF223046**	JN089034	JN089318	JN089274	JN089148
Physcomitrium pyriforme 1	Goffinet 4737	USA	CONN	JN089190	JN089233	JN088962	**EF173155**	JN089079	JN088993	**JN089035**	**JN089319**	**JN089275**	**JN089149**
Physcomitrium pyriforme 2	Goffinet 9276	USA	CONN	JN089191	JN089234	JN088963	JN089109	JN089080	JN088994	JN089036	JN089320	JN089276	JN089150
Physcomitrium sphaericum	Lüth 4283	France	Lüth[a]	JN089192	JN089235	JN088964	–	JN089081	JN088995	JN089037	JN089321	JN089277	JN089151
Pyramidula tetragona	Ros, Cano and Gallego	Morocco	MUR	JN089193	JN089236	JN088965	JN089110	JN089082	JN088996	JN089038	JN089322	JN089278	JN089152
Timmia megapolitana	Schofield 97957	Canada	DUKE	JN089194	JN089237	JN088966	–	JN089083	**AY908619**	**JN089039**	**JN089323**	**JN089279**	**JN089153**
Timmia norvegica	Vanderpoorten 4022	Switzerland	ULG	JN089195	JN089238	**DQ397184**	–	JN089084	JN088997	JN089040	JN089324	JN089280	JN089154

[a] Personal herbarium.
[b] IMSC: The International Moss Stock Center.

and cultured in 6 ml LB broth, plasmid vectors were extracted by QIAprep Spin Miniprep Kit (Qiagen, California, USA), and used as templates for sequencing using universal vector primers T7 and T3. Amplification of the *adk* and *ho* loci yielded two paralogs with incongruent phylogenetic signals and hence targeting of these loci was not pursued as part of this study.

2.3. Alignment and phylogenetic analyses

2.3.1. Sequence alignment

Sequences from different DNA regions were aligned separately with MUSCLE 3.8.31 (Edgar, 2004). For the three relatively fast loci, ITS, *atp*B–*rbc*L and *pet*D–N, alignments were made firstly in two portions (Funarioideae, and the remaining taxa), and then combined with profile techniques in MUSCLE. For each alignment, ambiguous regions were excluded by running GBLOCKS (Talavera and Castresana, 2007) on the server (http://molevol.cmima.csic.es/castresana/Gblocks.html) using the least stringent settings. Finally, all aligned regions were concatenated in PAUP* v4.0b10 (Swofford, 2003). The alignment is deposited on TreeBASE (http://www.treebase.org) (Submission S11826). For each locus, variable and parsimony-informative sites were estimated using MEGA 4 (Tamura et al., 2007).

2.3.2. Data partitioning

Partitioning of the data set may have a strong effect on the topology and estimates of nodal support (Brown and Lemmon, 2007; Li et al., 2008; McGuire et al., 2007). To explore the effect on the reconstruction of the relationships within the Funariaceae, we implemented six distinct partition schemes in model-based analyses. The data were partitioned a priori on the basis of gene identity, general biochemical or evolutionary constraints (e.g., codon position, intron and spacer). For each partition under the different schemes, the optimal nucleotide substitution model was chosen based on the Akaike Information Criterion (AIC; Akaike, 2002) using MrModeltest 2.3 (Nylander, 2004), which compares the 24 models supported by MrBayes, and jModelTest 0.1.1 (Posada, 2008), which compares the 88 substitution models that can be invoked in GARLI. Sequence characteristics and model selections for all data partitions are summarized in Table 2.

The six partition schemes mentioned above are as following: P1 (no partitioning); P2 (two data subsets: organellar sequences, nuclear sequences); P3 (three data subsets: partitioned by three genomes); P11 (11 data subsets: each gene in a separate subset, with *rps*4 divided into the gene and *rps*4–*trn*S spacer); P13 (13 data subsets: for *rps*4 and *rpl*2, the 1st and 2nd codon positions are separated from 3rd positions into separate subsets; each other locus treated as an individual subset); P15 (15 data subsets: for *rps*4 and *rpl*2, codon positions distributed into three partitions; each other locus treated as an individual subset).

For the likelihood analyses, AIC and Bayesian Information Criterion (BIC) were used to assess the optimal data partition model. In both approaches, the likelihood score estimated by Garli under each partitioning scheme is penalized by a function of the number of free parameters in the model. The model with the smallest AIC or BIC is considered the best. For the Bayesian analyses, Bayes factor (BF) was used to determine the optimal partitioning scheme. BF was calculated based on marginal likelihood, and the marginal likelihood in turn, is generated by Phycas 1.2.0 (Lewis et al., 2008) using the generalized SS method (Fan et al., 2010). BFs were compared one to each other for all partitioning models. If 2ln BF > 10, then the difference between the two models is considered to be significant (Kass and Raftery, 1995).

2.3.3. Phylogenetic analyses

Phylogenetic analyses were performed using maximum parsimony (MP), maximum likelihood (ML) and Bayesian inference (BI) methods. MP analyses were carried out with PAUP* version 4.0b10 (Swofford, 2003), heuristic searches were conducted with 1000 replicates of each 100 random sequence addition, tree-bisection–reconnection (TBR) branch swapping and Mul-Trees in effect. All characters were unordered and equally weighted, and gaps were coded as missing data. To assess node support, bootstrap analyses (Felsenstein, 1985) were performed using 1000 heuristic search replicates as described above.

Maximum likelihood analyses were carried out using GARLI-PART v0.97 (Zwickl, 2006), which allows for likelihood analysis

Table 2
Sequence characteristics and models chosen for each data partition.

Gene	*L*	All taxa		Funarioideae		Lineage III		Model selected by MrModeltest	Model selected by jModelTest
		Vs (%)	PIs (%)	Vs (%)	PIs (%)	Vs (%)	PIs (%)		
Nuclear gene ITS	593	327 (55.1)	267 (45.0)	137 (23.1)	94 (15.9)	96 (16.2)	58 (9.8)	K80 + I + Γ	TrN + I + Γ
Chloroplast genes	3109	1171 (37.7)	782 (25.2)	507 (16.3)	322 (10.4)	302 (9.7)	156 (5.0)	GTR + I + Γ	TPM1uf + I + Γ
*atp*B–*rbc*L	630	258 (41.0)	188 (29.8)	104 (16.5)	68 (10.8)	53 (8.4)	24 (3.8)	GTR + Γ	GTR + I + Γ
*pet*D–N	764	377 (49.3)	211 (27.6)	162 (21.2)	98 (12.8)	106 (13.9)	53 (6.9)	GTR + Γ	GTR + Γ
*psb*A–*trn*H	520	129 (24.8)	96 (18.5)	56 (10.8)	36 (6.9)	30 (5.8)	18 (3.5)	GTR + I + Γ	GTR + I + Γ
*rps*4	668	201 (30.1)	136 (20.4)	84 (12.6)	54 (8.1)	51 (7.7)	24 (3.6)	GTR + Γ	TVM + I + Γ
*rps*4 1st	203	45 (22.2)	32 (15.8)	18 (8.9)	15 (7.4)	11 (5.4)	7 (3.4)	HKY + Γ	TIM1 + I + Γ
*rps*4 2nd	203	35 (17.2)	22 (10.8)	14 (6.9)	8 (3.9)	13 (6.4)	7 (3.4)	GTR + Γ	TIM3 + I + Γ
*rps*4 1st + 2nd	406	80 (19.7)	54 (13.3)	32 (7.9)	23 (5.7)	24 (5.9)	14 (3.4)	HKY + I + Γ	TPM1uf + I + Γ
*rps*4 3rd	203	85 (41.9)	59 (29.1)	33 (16.3)	20 (9.9)	18 (8.9)	6 (3.0)	GTR + Γ	GTR + Γ
*rps*4–trnS	59	36 (61.0)	23 (39.0)	19 (32.2)	11 (18.6)	9 (15.3)	4 (6.8)	GTR + Γ	TIM1 + Γ
*trn*L–F	527	206 (39.1)	151 (28.7)	101 (19.2)	66 (12.5)	62 (11.8)	37 (7.0)	HKY + Γ	TVM + I + Γ
Mitochondrial genes	2955	614 (20.8)	419 (14.2)	189 (6.4)	100 (3.4)	115 (3.9)	46 (1.6)	GTR + I + Γ	TVM + I + Γ
*atp*1–*trn*W	744	161 (21.6)	89 (12.0)	34 (4.6)	22 (3.0)	22 (3.0)	13 (1.7)	HKY + Γ	TVM + I + Γ
*nad*2–*trn*G	685	126 (18.4)	89 (13.0)	47 (6.9)	24 (3.5)	25 (3.6)	10 (1.5)	GTR + Γ	TVM + I + Γ
*rpl*2	780	171 (21.9)	132 (16.9)	56 (7.2)	30 (3.8)	38 (4.9)	13 (1.7)	GTR + Γ	GTR + I + Γ
*rpl*2 1st	260	61 (23.5)	47 (18.1)	20 (7.7)	11 (4.2)	13 (5.0)	3 (1.1)	HKY + Γ	TPM1uf + I + Γ
*rpl*2 2nd	260	53 (20.4)	43 (16.5)	20 (7.7)	10 (3.8)	14 (5.4)	5 (1.9)	HKY + I	TVM + I + Γ
*rpl*2 1st + 2nd	520	114 (21.9)	90 (17.3)	40 (7.7)	21 (4.0)	27 (5.2)	8 (1.5)	HKY + Γ	TVM + I + Γ
*rpl*2 3rd	260	57 (21.9)	42 (16.2)	16 (6.2)	9 (3.5)	11 (4.2)	5 (1.9)	GTR	TVM + I + Γ
*rps*7–*atp*6	746	156 (20.9)	109 (14.6)	52 (7.0)	24 (3.2)	30 (4.0)	10 (1.3)	HKY + Γ	TPM1uf + I + Γ
Organelle genes	6064	1785 (29.4)	1201 (19.8)	696 (11.5)	422 (7.0)	417 (6.9)	202 (3.3)	GTR + I + Γ	TPM1uf + I + Γ
Combined	6657	2112 (31.7)	1735 (26.1)	833 (12.5)	516 (7.8)	513 (7.7)	260 (3.9)	GTR + I + Γ	TVM + I + Γ

Note: *L* = length of partition (bp); Vs = variable sites (bp); PIs = parsimony informative sites (bp). Models were chosen based on the data including all taxa.

with partitioned data sets. For every GARLI analysis, the program was run twice, each with five replicates, using the default settings. The topology with the highest likelihood score was chosen as the best tree. Statistical supports for branches were obtained via non-parametric bootstrapping with 100 pseudoreplicates.

Bayesian inference was conducted using MrBayes version 3.0b4 (Ronquist and Huelsenbeck, 2003). The analysis was performed with two runs, each having four chains, with trees and parameters sampled every 1000th generation. For partitioned analyses, parameters were unlinked among the partitions, so that model parameters are estimated independently for the various partitions. In all analyses, branch lengths and topology were linked. Burn-in and convergence were assessed using the likelihood of the runs plotted against generations using Tracer v.1.5 (Rambaut and Drummond, 2009). Posterior probabilities (PP) were estimated by sampling trees from the PP distribution. Trees were summarized after removing the burn-in samples. Finally, a 50% majority-rule consensus tree was built in MrBayes.

Preliminary analyses of 5 million (M) generations indicated that the less partitioned (P1, P2, and P3) models reached stationarity quickly in comparison to the more partitioned models (P11, P13, and P15), in which likelihood parameters failed to converge across runs during the entire analysis. In addition, the three most complicated models had unreasonably longer total tree length (TL), ranging from 2.49 to 5.94 (versus 0.73–0.95 in the three simpler models). Performing complex data partitioning schemes raises the possibility of chains trapped on local optima (Brandley et al., 2005; Marshall, 2010; Nylander et al., 2004; Ward et al., 2010). To avoid this problem Marshall (2010) and Brown et al. (2010) suggested placing a shorter prior on the mean branch length. Brown et al. (2010) provided a formula to calculate the exponential rate parameter for the branch-length prior ($\lambda = \ln(0.5)/\overline{brl}$), where $\overline{brl}$ is the average branch length obtained by TL/number of branches. In our analyses, we used 0.94 (result of 15-partition analysis in GARLI) as the appropriate gross tree length, and inferred the value $\lambda = 63$ (by default, $\lambda = 10$ in MrBayes). After setting a shorter prior on the average branch length using prset applyto = (all) brlenspr = unconstrained: exponential (63), all parameters converged after a short burn-in stage. In addition, the TLs were shorter and likelihood scores higher. Ultimately we ran 10 M, 20 M, or 80 M generations for each dataset, depending on the number of partitions used in the analyses.

2.4. Morphological characters scoring

We characterized all exemplars for five morphological characters, which are typically used to define the genera within the Funariaceae: (1) the architecture of the peristome, (2) the length of the seta that determines whether the capsule is immersed or emergent, (3) the inclination of the capsule, (4) the shape of calyptra and (5) the complexity of the annulus. Character states were obtained from Fife (1985) and vouchers. We did not reconstruct ancestral character states, as the taxon sampling is largely incomplete. Instead the distribution of the character states among terminal taxa of the Funarioideae in a parsimony bootstrap 50% majority-rule consensus tree is shown to illustrate the morphological context underlying the phylogenetic hypothesis presented here. These morphological characters are shown in Supplementary Fig. S3.

2.5. Alternative hypothesis test

To assess the strength of the conflicts between traditional generic circumscriptions and those emanating from the phylogenetic inferences, as well as the conflicting results generated from different phylogenetic inference methods, we compared the likelihoods of alternative hypotheses against that of the unconstrained ML tree using the Kishino–Hasegawa (KH) test (Kishino and Hasegawa, 1989), the Shimodaira–Hasegawa (SH) test (Shimodaira and Hasegawa, 1999), the weighted KH and SH (namely WKH and WSH) tests, the approximately unbiased (AU) test (Shimodaira, 2002) and also the expected-likelihood weight (ELW) approach (Strimmer and Rambaut, 2002). The alternative hypotheses are: (1) the one-partition Bayesian tree, (2) the single MP tree generated from the parsimonious analysis, (3) the tree with the highest likelihood estimated with the constraint that *Physcomitrella* are monophyletic, (4) the ML tree with *Physcomitrium* constrained as monophyletic, (5) the ML tree with *Entosthodon* constrained as monophyletic, and (6) the ML tree with *Entosthodon* in linage III constrained as monophyletic. The constrained trees (with certain taxa set up as monophyletic and others left as polytomy) were built in Mesquite v2.74 (Maddison and Maddison, 2010), and then optimized in GARLI-PART v0.97 under the 15-partition model. The best tree of 10 GARLI replicates was chosen for comparison. All the tests were conducted with TREE-PUZZLE 5.2 (Schmidt et al., 2002) and CONSEL v 0.1k (Shimodaira and Hasegawa, 2001). Site-wise log-likelihoods were estimated by TREE-PUZZLE, and then were also used as input data for CONSEL.

Additionally, we also used a parametric bootstrapping method, the Swofford–Olsen–Waddell–Hillis (SOWH) test (Goldman et al., 2000) to compare the six alternative hypotheses mentioned above. The SOWH test is considered to have more power and be able to avoid type I error when model parameters are accurately provided (Buckley, 2002). Due to computational limitations, a faster ML based program RAxML v7.0.4 (Stamatakis, 2006) was used to infer the tree and parameters. First we constrained the tree such that a specific group was monophyletic, and optimized the tree topology, branch lengths and model scores from the original data (GTR + I + Γ model, 15-partition). Then we simulated 100 replicate datasets based on this optimized tree and parameters using SEQ-GEN v1.3.2 (Rambaut and Grassly, 1997). Later on, for each one of these datasets, we conducted two likelihood searches, one to find the optimal unconstrained tree, the other to find the optimal constrained tree. The distribution of log likelihood differences between the "optimal constrained" and "optimal unconstrained" trees were determined and used for evaluating the significance of difference between the two topologies. To perform the calculations, scripts were created to automate the procedures when running RAxML, Python 2.7 was used to extract executable RAxML data matrix from SEQ-GEN output files, and a program (exlikelihood.exe, available on request from the first author) written in Fortran 90 was made for automatically extracting likelihood scores from RAxML results. The distributions of likelihood differences were plotted in Excel. Ultimately the difference between the likelihood scores of the unconstrained and constrained trees inferred using the original dataset was compared to the distribution of likelihood differences between trees inferred from the simulated datasets.

2.6. Phylogenetic conflict visualization

We assessed whether the lack of resolution within the tree resulted from inadequacy of the data (either due to lack of variation or inherent conflict among the data) using likelihood mapping and then located the conflict on the phylogenetic tree by reconstructing a supernetwork.

In order to visualize the content of phylogenetic signals, we performed likelihood mapping (Strimmer and Von Haeseler, 1997) analyses for all-taxa and lineage III datasets using the program TREE-PUZZLE 5.2 (Schmidt et al., 2002). The analysis visualizes phylogenetic content of aligned sequences by plotting probability

vectors of any quartets of taxa in an equilateral triangle. Results are also shown with a partitioned triangular graph. The three tips of the triangle represent the percentage of quartets well resolved. Three rectangles on the sides represent quartets with network evolution (conflicting signal). The central region of the triangle represents star-like evolution (noisy signal). The analyses consisted of sampling 20,000 quartets under the GTR + I + Γ model.

The trees inferred from the combined organellar data and from the nuclear ITS sequences exhibited topological incongruence. To visualize these, we generated a supernetwork using SplitsTree 4.11.3 (Huson and Bryant, 2006). We used the Z-closure option, mean edge weights, and setup splits transformation = Equal Angle, and set other parameters as default. The input trees used to construct the supernetwork were the 50% majority-rule consensus of 1000 MP bootstrap searches.

3. Results

3.1. Alignment of DNA sequences

A total of 381 sequences were newly generated for this study. Fifteen sequences are missing from the matrix, but these include nine for the chloroplast *pet*D–N locus which identifies a structural rearrangement lacking in the Gigaspermaceae and Timmiaceae (Goffinet et al., 2007). Alignment of the 10 loci yielded a combined data matrix of 9219 bp, which following the exclusion of ambiguous regions was reduced to 6657 bp prior to the analyses. This matrix is composed of 47% (3109 bp) chloroplast, 45% (2955 bp) mitochondrial, and 8% (593 bp) nuclear sites (Table 2). The 10 loci exhibit various degrees of variability with the nuclear locus (ITS) more variable than any of the five chloroplast loci, which in turn are more divergent than the four mitochondrial loci. Compared to combined mitochondrial loci, the rate of evolution of the alignable and analyzed portion of the nuclear ITS is 2.6, 3.6 and 4.1 times higher across all taxa, the Funarioideae and lineage III, respectively (Table 2).

3.2. Data partitioning

Under the likelihood criterion, P15 was selected as the best-fit partition scheme. AIC and BIC values decreased with increasing number of partitions, and the most partitioned model obtained the smallest score (Table 3). By contrast, Under the Bayesian criterion, selection of a partition scheme based on BF favored P13 (Table 5). Bayes factors indicated that the less partitioned model P1 was better than the more partitioned models P2 and P3, and the most partitioned model P15 did not fit the best (Tables 4 and 5).

3.3. Phylogenetic reconstruction

To assess incongruence among the three genomic compartments, we compared trees and nodal support values inferred from each set of loci. Incongruence among data sets is revealed by topological conflicts supported by BS values ⩾70% as described in Mason-Gamer and Kellogg (1996) in both data partitions. No ingroup conflict was observed between the chloroplast and mitochondrial data, which were thus combined. Comparisons of trees inferred from organellar and nuclear loci revealed three topological conflicts, of which only one was significant and thus considered indicative of incongruence. When the taxon causing the incongruence, *Physcomitrium sphaericum*, was excluded the data sets were fully congruent, and the relationships among other lineages were the same as when this taxon was included. Hence, data from the three compartments were combined and all taxa were included. Eleven of the 13 analyses (by different methods and/or under different partition schemes), including all 6 ML and 5 BI analyses yielded identical topology. The MP analysis as well as the Bayesian inference under the partition scheme P1 yielded distinct trees that differed in affinities of *Discelium nudum* (in MP tree) and/or *Physcomitrium pyriforme* 1 (see Supplementary Figs. S1 and S2). In neither case, however, were these optimal relationships strongly supported (Table 6). A phylogram (15-partition ML tree) of one of the 11 congruent trees obtained from the other analyses is shown in Fig. 1. The Funariaceae are resolved as a robust (BS = 100%, PP = 1.00) monophyletic group (node 13) and share a unique common ancestor with the Encalyptaceae (82% < BS < 93% under ML, node 9; Table 6). The Disceliaceae are resolved as sister to Funariaceae + Encalyptaceae (node 8; Table 6), but with weak (BS < 70%) or moderate (70% < BS < 90%) bootstrap support. Both nodes 8 and 9 have strong posterior probabilities (PP > 0.95) in Bayesian analyses.

The two subfamilies of Funariaceae, the Pyramiduloideae and Funarioideae, were resolved as maximally supported sister lineages (BS = 100%, PP = 1.00) in all analyses. Within the Funarioideae the species are distributed among three maximally

Table 3
Summary of maximum likelihood analyses. Ln*L* is the best likelihood score estimated by GARLI under each partition model. The values in bold indicate the optimal partitioning strategy selected by AIC and BIC. Total tree length of each ML tree was calculated by PAUP.

Partition model	TL	Ln*L* (L)	No. parameters (P)	AIC	BIC
P1	0.90	−33049.4926	9	66116.9852	66133.0429
P2	0.87	−32654.2743	15	65338.5486	65342.6063
P3	0.90	−32198.7203	25	64447.4406	64431.4983
P11	0.94	−31896.0447	106	64004.0894	63826.1471
P13	0.94	−31819.1660	123	63884.3320	63672.3897
P15	0.94	−31801.0680	141	**63884.1360**	**63636.1937**

Note: TL = total tree length; AIC = −2L + 2P; BIC = −2L + log(*n*) P, *n* is the sample size.

Table 4
Summary of Bayesian analyses. Bayesian parameters are based on combination of two runs. Marginal likelihoods were obtained by generalized SS methods for evaluating the six partitioning strategies.

Partition model	Generations	Burn-in	Mean LnL	Mean TL	Marginal likelihood
P1	20 M	2 M	−35464.399	0.73	−41905.2099
P2	20 M	2 M	−32706.276	0.91	−42312.3975
P3	20 M	2 M	−32260.028	0.95	−42117.1068
P11	20 M	2 M	−31994.611	0.95	−41726.6368
P13	40 M	4 M	−31934.327	0.95	−41670.3686
P15	80 M	8 M	−31924.581	0.95	−41783.2966

Note: TL = total tree length.

Table 5
2ln Bayes factor comparisons of six partitioning strategies. The strategies are named by partition numbers (P1–P15). Result values were calculated by marginal likelihood of more complex model minus less complex model. A positive value indicates evidence against alternative hypotheses. Bold value indicates the optimal partitioning strategy.

	Partitioning strategies					
	P15	P13	P11	P3	P2	P1
P1	243.8266	**469.6826**	357.1462	−423.7938	−814.3752	–
P2	1058.2018	**1284.0578**	1171.5214	390.5814	–	
P3	667.6204	**893.4764**	780.9400	–		
P11	−113.3196	**112.5364**	–			
P13	−225.8560	–				
P15	–					

Table 6
Support values under different model partitioning strategies (P1–P15), based on MP, ML bootstraps and Bayesian PPs. Bootstrap supports under 50% are shown by "–". NP indicates node not present in tree. Shaded values indicate a node receiving strong support (BS > 90 or PP > 0.95). Bold values are from ML and BI analyses under the optimal partitioning strategies. Node names correspond to Fig. 1.

Node	MP	ML-P1	ML-P2	ML-P3	ML-P11	ML-P13	ML-P15	BI-P1	BI-P2	BI-P3	BI-P11	BI-P13	BI-P15
Node 4	98	95	95	98	96	97	**93**	1.00	1.00	1.00	1.00	**1.00**	1.00
Node 8	69	67	81	74	65	77	**69**	1.00	0.99	1.00	1.00	**1.00**	1.00
Node 9	NP	93	88	88	84	84	**82**	0.99	1.00	1.00	1.00	**1.00**	1.00
Node 10	94	99	100	100	100	100	**100**	1.00	1.00	1.00	1.00	**1.00**	1.00
Node 12	97	90	92	95	88	92	**95**	1.00	1.00	1.00	1.00	**1.00**	1.00
Node 18	98	97	99	98	97	98	**99**	1.00	1.00	1.00	1.00	**1.00**	1.00
Node 19	100	90	93	93	90	92	**91**	1.00	1.00	1.00	1.00	**1.00**	1.00
Node 23	71	84	88	76	77	79	**79**	1.00	0.99	1.00	0.99	**0.99**	0.99
Node 24	95	96	95	93	92	93	**96**	1.00	1.00	1.00	1.00	**1.00**	1.00
Node 26	76	72	78	71	65	72	**68**	1.00	0.96	0.97	0.96	**0.96**	0.96
Node 27	99	98	100	100	100	100	**99**	1.00	1.00	1.00	1.00	**1.00**	1.00
Node 28	–	53	55	57	53	54	**51**	0.98	0.99	0.98	0.98	**0.98**	0.98
Node 31	93	95	93	97	93	90	**92**	1.00	1.00	1.00	1.00	**1.00**	1.00
Node 33	74	70	53	58	62	53	**60**	1.00	0.85	0.86	0.87	**0.88**	0.88
Node 34	99	99	98	98	97	99	**99**	1.00	1.00	1.00	1.00	**1.00**	1.00
Node 35	NP	–	–	–	–	–	–	NP	0.76	0.65	0.82	**0.84**	0.82
Node 36	NP	–	–	–	–	–	–	NP	0.92	0.81	0.93	**0.94**	0.93
Node 38	95	96	94	96	95	93	**94**	1.00	1.00	1.00	1.00	**1.00**	1.00
Node 39	88	87	89	86	88	85	**86**	1.00	1.00	1.00	1.00	**1.00**	1.00

supported clades (BS = 100%, PP = 1.00), which will hereafter be referred to as lineage I, II and III. Lineage I comprises three species of *Funaria* s. str. Lineage II includes the monospecific genus *Funariella* and two species of *Entosthodon*. Lineage III accommodates all other Funarioideae sampled in this study. Of the three speciose genera, only *Funaria* s. str. is recovered as monophyletic. Members of *Entosthodon* and *Physcomitrium* are scattered across several well-supported clades. The relationships among these clades are not supported (Fig. 1): nodes 35 and 36 lack any BS or strong PP support and node 28 received no BS but high PP.

Even the small genus *Physcomitrella* is highly polyphyletic with its three species resolved within three different clades (Fig. 1). *P. patens* shares a common ancestor with *Aphanorrhegma serratum*, *P. sphaericum*, and *Physcomitrium immersum*. *Physcomitrella readeri* is strongly supported in all analyses as the sister taxon to the monospecific genus *Bryobeckettia* (node 24, Table 6). Together these taxa compose the sister group (node 23) to a maximally supported clade comprising *Physcomitrella magdalenae*, *Physcomitrium lorentzii*, *P. pyriforme* 2 and *Entosthodon fascicularis*.

3.4. Morphological characters mapping

Five characters were scored for each exemplar and superimposed onto the MP 50% bootstrap consensus tree (Fig. 2). The combination of character states is constant only within lineage I (i.e., *Funaria*), which also uniquely exhibits a compound revoluble annulus. Lineage II and III are heterogeneous both in terms of character combinations and individual character states (except for the lack of a complex annulus; Fig. 2). Peristomes are lacking in several taxa distributed across lineages II and III and lineages therein. Similarly sessile capsules occur in several unrelated taxa or lineages, and calyptra shape is slightly more conserved within lineages.

3.5. Alternative hypothesis test

Multiple non-parametric bootstrapping methods showed that constraining *Physcomitrella*, *Physcomitrium*, *Entosthodon* or only the *Entosthodon* within lineage III as monophyletic always resulted in topologies that did not fit the data significantly better ($P < 0.01$) than the unconstrained ML topology under any test (Table 7). By contrast, none of the tests rejected the topologies yielded by the MP analysis and BI inference from the single partition data set (Table 7).

The parametric bootstrapping method (the SOWH test) indicated that with *Physcomitrella* constrained as monophyletic yielded a log-likelihood that is 334.5 units worse than the unconstrained optimal tree. This difference is significant at the 0.01 level (4.8 units), so the monophyly of *Physcomitrella* should thus be rejected. Similarly, neither the MP (13.0 versus 4.0) and the one-partition BI tree (4.5 versus 3.2) nor any of the other three constrained trees (*Entosthodon* monophyly, 649.8 versus 3.2; *Physcomitrium* monophyly, 419.5 versus 2.4; *Entosthodon* in lineage III monophyly, 230.2 versus 3.2) could be accepted by the SOWH tests (Fig. 3).

3.6. Conflict visualization

Likelihood mapping (Fig. 4) reveals that the relationships of quartets of taxa in lineage III are less often resolved than of those taxa sampled across the entire tree (92.8% versus 95.0%, summary of numbers in the three corners). The sequences from lineage III carry a proportion of conflicting signal similar to that of the entire data set (3.2% versus 3.3%, summary of numbers in peripheral rectangles between corners). The proportion of noise in either data set (4.0% versus 1.7%, in central triangle) is well below the "high" threshold of 20–30% (Lemey et al., 2009), suggesting that both datasets are suitable for phylogenetic reconstructions.

The trees inferred from the combined organellar data and from the nuclear ITS exhibited topological incongruence. Because ITS could not be sequenced for all taxa (42 versus 44), a supernetwork (Huson et al., 2004), which can incorporate partial trees, was reconstructed. One competing split between the organellar and nuclear based inference pertains to the position of the Disceliaceae (Fig. 5). This taxon is sister to Encalyptaceae in the organellar gene tree (BS = 74%) and belongs to a collapsed clade containing Funariaceae + Encalyptaceae and Gigaspermaceae in the ITS tree. Within lineage III, two conflicts occur: *P. pyriforme* 2 is sister to *P. lorentzii* + *P. magdalenae* (BS = 81%) in the organellar gene tree but sister to *E. fascicularis* (BS = 60%) in the ITS tree, and *P. sphaericum* is sister to *P. immersum* (BS = 90%) in the organellar gene tree, but sister to *A. serratum* (BS = 88%) in the nuclear ITS tree. No conflicts were observed along the backbone of lineage III.

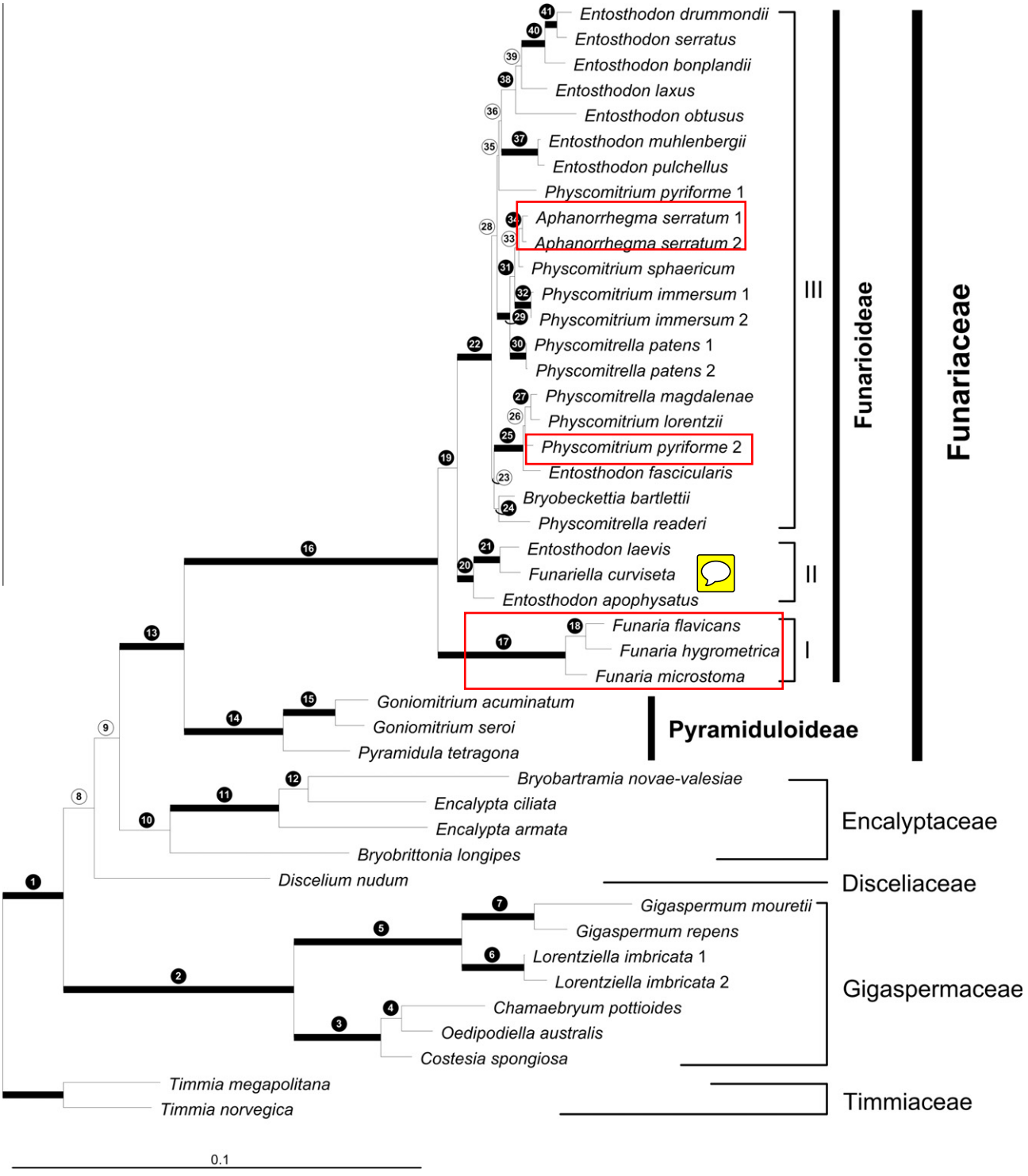

Fig. 1. Maximum-likelihood phylogram estimated by GARLI based on the combined 10-gene dataset under the partition scheme P15. Thickened branches indicate receiving 100% MP, ML bootstrap and 1.00 BI posterior probability supports. Supports of other branches are listed in Table 6. Nodes are numbered above branches. Filled circles indicate nodes receiving strong supports (MP and ML > 90% and BI > 0.95). Empty circles indicate nodes with only moderate (70% < MP and ML < 90% and/or 0.90 < BI < 0.95) to weak (MP and ML < 70% and/or BI < 90%) supports in one or multiple analyses. Group names are listed on the right side of the tree.

4. Discussion

The Funariaceae compose a diverse lineage of mosses united by the shape of their paraphyses, and displaying a rather uniform vegetative body plan in contrast to a broad amplitude in the architectural complexity of the sporophyte. The generic classification has hence reflected mostly patterns in the variation in the mode of dehiscence, peristome, seta length, and symmetry of the capsule (Fife, 1985). Phylogenetic inferences from 10 loci from all three genomic compartments support the monophyly of the Funariaceae sensu (Goffinet et al., 2009) as well as a sister group relationship between the Pyramiduloideae and Funarioideae as early proposed

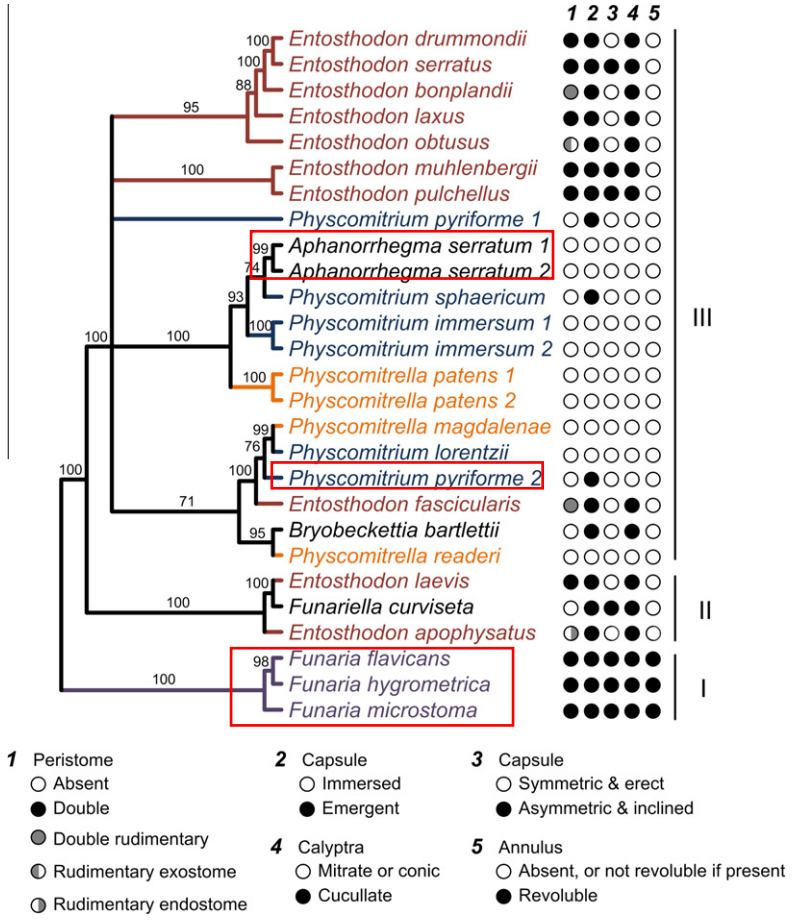

Fig. 2. Parsimony 50% majority-rule bootstrap consensus tree based on the combined 10-gene dataset. A partial cladogram is shown here (Funarioideae only). Numbers above branches are bootstrap values (>50%). Selected morphological characters for each taxon are listed beside the tree. Taxa and branches are colored based on genera.

Table 7
Comparison between the ML tree (Fig. 1) and the alternative hypotheses. *P*-values were estimated with TREE-PUZZLE and Consel. The sign "+"indicates the alternative topology differing significantly (*P*-value at 0.01) from the ML tree, and should be rejected.

Hypothesis	TREE-PUZZLE					Consel				
	$\Delta \log L$	S.E.	KH	SH	ELW	KH	SH	WKH	WSH	AU
Bayesian tree based on one partition	0.90	7.00	0.472	0.899	0.412	0.443	0.896	0.443	0.882	0.553
Most parsimonious tree	11.36	9.98	0.140	0.688	0.063	0.129	0.688	0.104	0.327	0.077
Physcomitrella monophyletic ML tree	358.33	41.13	0.000+	0.000+	0.000+	0.000+	0.000+	0.000+	0.000+	<0.001+
Physcomitrium monophyletic ML tree	441.94	46.09	0.000+	0.000+	0.000+	0.000+	0.000+	0.000+	0.000+	<0.001+
Entosthodon monophyletic ML tree	640.63	54.02	0.000+	0.000+	0.000+	0.000+	0.000+	0.000+	0.000+	<0.001+
Entosthodon in lineage III monophyletic ML tree	240.68	32.95	0.000+	0.000+	0.000+	0.000+	0.000+	0.000+	0.000+	<0.001+

by Werner et al. (2007) and 2) suggest a polyphyletic nature of *Entosthodon*, *Physcomitrella* and *Physcomitrium* but support the monophyly of *Funaria* sensu (Fife, 1985). These hypotheses are robust and cannot be considered an artifact of the data, the method of analysis or reflect hybridization, and therefore unambiguously suggest that most sporophytic characters central to the generic classification of the Funariaceae are homoplasious and hence poor indicators of phylogenetic affinities.

4.1. Validity of the new phylogenetic hypotheses

The robustness of the branches decreases along the backbone of the tree with the relationships within the crown group of the Funarioideae (i.e., lineage III) remaining largely unresolved. Phylogenetic ambiguity due to short internal branches characterizes various lineages of bryophytes (e.g., Hypnanae (Shaw et al., 2003); Marchantiidae (Wheeler, 2000); Bryaceae (Holyoak and Pedersen, 2007)) and vascular plants (e.g., seed plants (Burleigh and Mathews, 2004); early angiosperms (Soltis et al., 2005); Saxifragales (Jian et al., 2008); Brassicaceae (Koch et al., 2007)). The lack of resolution is due to either soft or hard polytomies. A soft polytomy is due to a number of artificial factors, such as inadequate data or taxa sampling, low sequence variation rates, gene conflicts caused by hybridization, or inappropriately applied phylogenetic methods and substitution models (Whitfield and Kjer, 2008; Whitfield and Lockhart, 2007). In contrast, a hard polytomy is caused by a rapid radiation resulting in much shorter immediate internal branches. We rule out below that the lack of robust phylogenetic resolution within the Funarioideae and in particular its crown group (i.e., lineage III) results from a priori limited or inadequate data, methodological artifacts or recurrent hybridization, and is indeed caused by a rapid radiation.

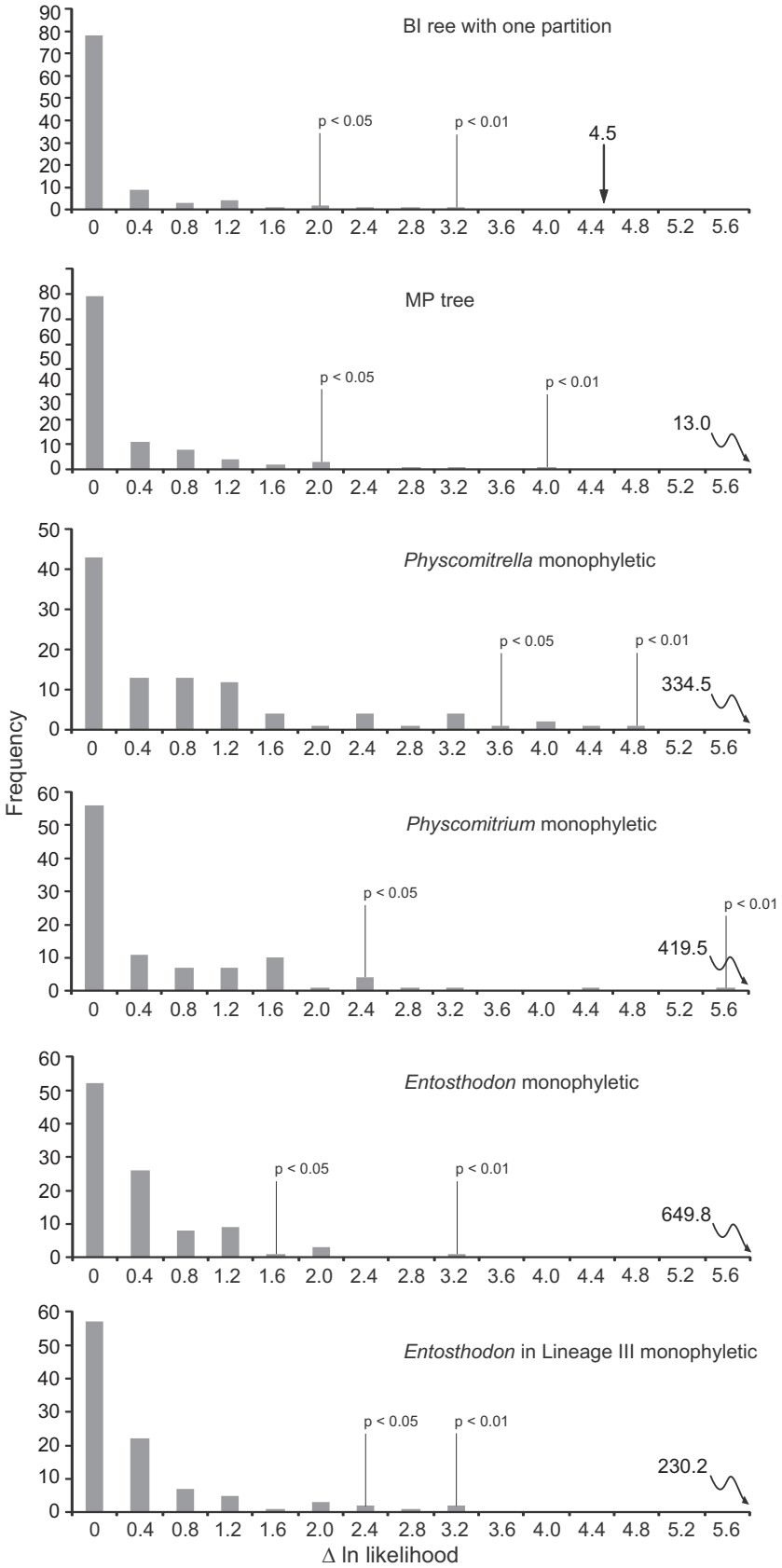

Fig. 3. The distributions for the SOWH (parametric bootstrapping) tests of the six alternative topologies. The histogram shows the distribution of 100 replicates. The 1%, 5% significance levels and the observed log-likelihood difference were shown for each hypothesis in the chart (see text for details).

Of the 6657 characters sampled, 1735 (26.1%) are potentially parsimony informative, and 260 (3.9%) are variable and not autapomorphic within the crown group of the Funarioideae (i.e., lineage III). Furthermore, likelihood mapping suggests that the

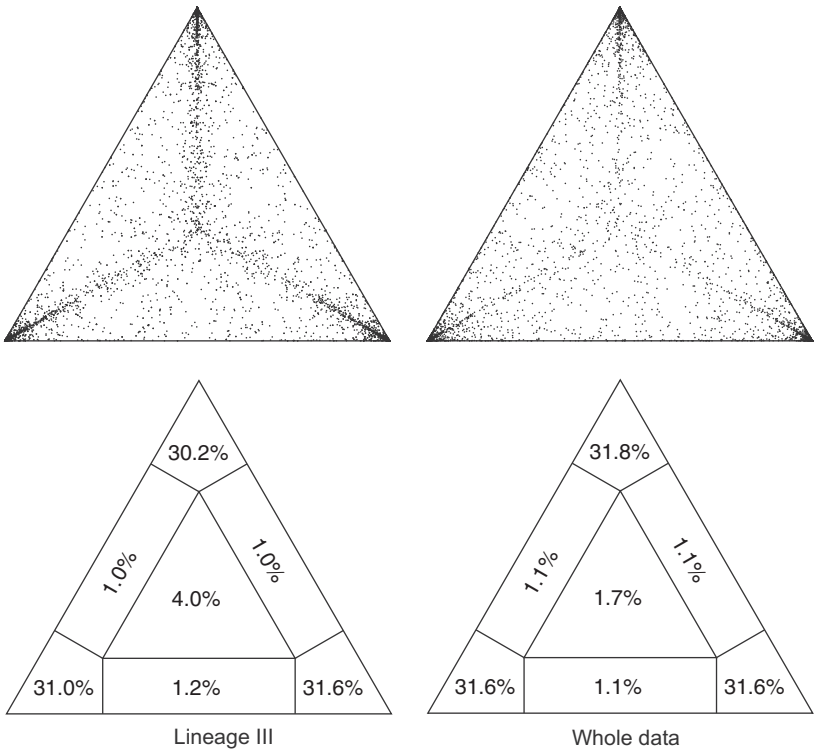

Fig. 4. Likelihood mapping results produced by TREE-PUZZLE based on datasets of Funarioideae lineage III (left), and all taxa sampling (right).

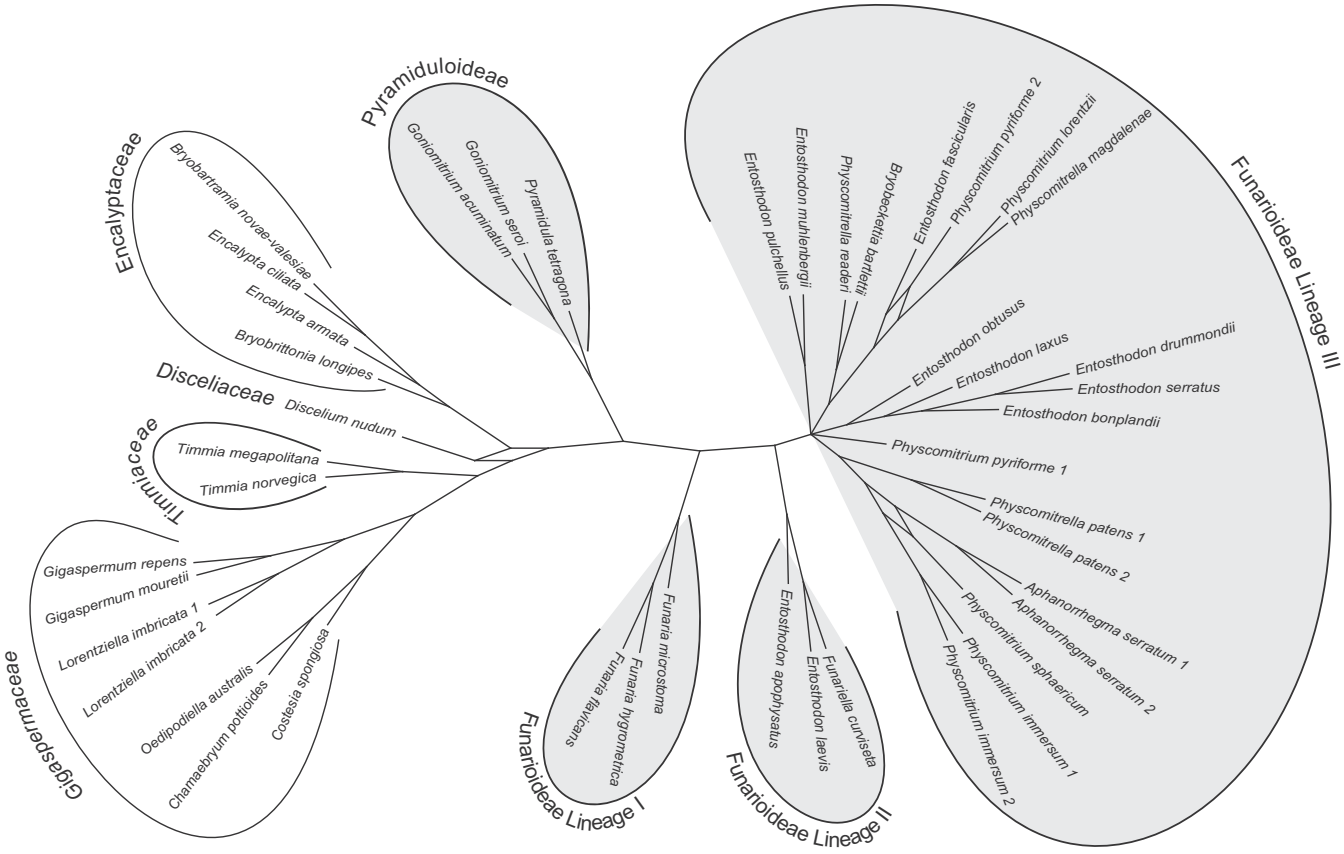

Fig. 5. Supernetwork of Funariaceae constructed from the organellar and nuclear gene trees using SplitsTree 4.11.3. Bipartitions occurring in more than 50% of 1000 parsimonious bootstrap replicates are shown. Boxes indicate incongruence. Clades are labeled as in Fig. 1. Gray-shaded taxa are members of Funariaceae.

proportion of resolved relationships is the same when using the 1735 characters for any four taxa or only 259 characters for a quartet of exemplars within lineage III. The data sampled should thus have been sufficient and adequate for inferring a robust phylogenetic hypothesis. Failure to resolve the relationships clearly suggest that more extensive sampling of loci will, however, be necessary.

The topology of the tree and the robustness of the branches may also be sensitive to the analytical methods, and in particular to the models of substitution applied for likelihood or Bayesian reconstructions (Brown and Lemmon, 2007; Li et al., 2008; McGuire et al., 2007). Nucleotide sequences from different genomes, genes under distinct selection constraints and different codon positions may differ in their evolutionary rate and substitution pattern (Drouin et al., 2008; Mower et al., 2007). For phylogenetic analyses, combining data blocks with homogeneous substitution rates is a reasonable strategy to accommodate sequence heterogeneity (Li et al., 2008). Both simulated and empirical datasets showed that partitioning improves likelihood scores and support values (Brandley et al., 2005; Brown and Lemmon, 2007; Castoe et al., 2004; Caterino et al., 2001; Pupko et al., 2002), in addition, partitioning also affects tree topologies (Brandley et al., 2005; Li et al., 2008; Ward et al., 2010). Partitioning the data sampled here greatly improved the Log likelihood scores in both Likelihood and Bayesian analyses (Tables 3 and 4), but most of the topologies remained the same (except for the one-partition BI tree, which was rejected by the SOWH test), and neither ML bootstrap percentages nor BI posterior probabilities benefited from increased partitioning (Table 6).

The robustness of a backbone phylogeny may also be weakened due to hybridization events, which may result in incongruent signals from different genetic sources. Potential for interspecific fertilization within the Funariaceae is well documented (e.g., von Wettstein, 1924) although its frequency in nature remains uncertain (Natcheva and Cronberg, 2004). Crossing between *P. patens*, *P. pyriforme* and *F. hygrometrica* yield hybrid sporophytes, but generally with smaller and aborted spores (Nicholson, 1931; Pettet, 1964; von Wettstein, 1932). Based on inferences from DNA sequence data, McDaniel et al. (2010) argued that hybridization may play a role in the diversification of the Funariaceae. In the present study, inferences from the organellar versus nuclear data suggest potential hybridizations within individual clades of lineage III (e.g., *P. pyriforme* 2 and *P. sphaericum*; Fig. 5) but not between major backbone clades within the Funariaceae. Phylogenetic evidence for hybridization as an explanation for the lack of resolution of relationships within the Funarioideae is lacking.

More likely the process accounting for the lack of phylogenetic resolution (hard polytomes) within lineage III may be a rapid and explosive diversification. With mutations scattered throughout the genome, insufficient time may separate two successive cladogenic events to allow for mutations to accumulate in discrete portions of the genome. Hence sampling even ten loci may fail to capture sufficient mutations to reconstruct the relationships, in particular when the diversification resulted in many new descendants as in the Funariaceae. In the ML tree (Fig. 1) the inferred length of the branches subtending nodes 23, 28, 35 and 36 is short (i.e., 0.0006, 0.0013, 0.0005 and 0.0006 substitutions per site) and accounted for by only 3.6, 7.8, 3.0 and 3.6 mutations across the 6657 bp dataset, respectively. As a result bootstrap percentages and posterior probabilities are low due to the scarcity rather than the conflicting nature of the data. Rapid and explosive radiations are thought to follow a founding effect in a new open environment, such as recently formed mountains, lakes and islands (Hughes and Eastwood, 2006; McCune, 1997; Schluter, 2000; Verheyen et al., 2003), or the evolution of a key innovation that confers a significant advantage resulting in an adaptive radiation (Bateman et al., 1998; Berenbaum et al., 1996; Bond and Opell, 1998; Freeman, 2000; Vamosi and Vamosi, 2011). No single morphological character or even life history trait unites species composing lineage III, and hence the trigger of the diversification remains unknown.

4.2. Evolution of the Funariaceae

The Funariaceae sensu (Fife, 1985) compose a strongly supported monophyletic entity with genera distributed between two main sister lineages treated by Werner et al. (2007) as the Funarioideae and Pyramiduloideae. The latter comprises only six species (Crosby et al., 1999) accommodated into two genera, *Goniomitrium* and *Pyramidula*, which differ from the Funarioideae by the large (typically >50 μm), ovoid to elliptical spores and the pleated or angled (versus smooth) calyptra (Fife, 1985).

Within the Funarioideae, three species of *Funaria* arose from a unique ancestor that is sister to the remainder of the subfamily. These three species share a compound and revoluble annulus, which Fife (1985) viewed as diagnostic of *Funaria*. Although our sampling includes only three of the potentially 30 taxa assigned to *Funaria* (Fife, 1982), none of the species of *Entosthodon* occasionally placed in *Funaria* (e.g., *Entosthodon serratus* (McIntosh, 2007)) on the basis of their asymmetric capsule are recovered within this lineage. Fife's (1985) concept of *Funaria* has not been widely adopted; in fact, only Brugués and Ruiz (2010) seem to explicitly segregate *Entosthodon* based on the lack of the complex annulus, rather than on the shape of the capsule as is more commonly proposed (McIntosh, 2007). *Funaria* may also be characterized by the sulcae on the dry capsule, which are due to an alternation of bands of thick and thin-walled exothecial cells and by its double peristome. The exostome teeth are united at their apex, and an endostome is composed of well developed (*F. hygrometrica*) or truncated (*F. flavicans*) segments, which may even be reduced to a low membrane (*Funaria microstoma*).

The remaining Funarioideae compose a well supported monophyletic lineage within which *Entosthodon* sensu Fife (1985), *Physcomitrella* and *Physcomitrium* are clearly polyphyletic. Although the data fail to fully resolve the relationships within the lineage, they are sufficient to reject with confidence the monophyly of these genera based on non-parametric or parametric statistical tests (Table 7). Already Fife (1985) had shown based on phenetic analyses of 28 sporophytic and nine gametophytic characters that the *Entosthodon* and the *Physcomitrium* clusters were heterogeneous due to the inclusion of *Brachymeniopsis* or *Aphanorrhegma* and *Physcomitrella*, respectively. Given the multitude of monospecific genera in the Funariaceae (i.e., eight) it may not be surprising that at least some of these arose within speciose genera, which are thereby rendered polyphyletic. Affinities of *Aphanorrhegma* to *P. immersum* and *P. sphaericum* as suggested by Fife (1985) are recovered here. In addition, *Funariella*, the last monospecific genus established (Sérgio, 1988) is nested between two species of *Entosthodon*. However, the polyphyly of *Entosthodon* and *Physcomitrium* is not only caused by the inclusion of monospecific genera: species of *Physcomitrella* are scattered across the tree, and even pruning them does not recover monophyly for either *Entosthodon* or *Physcomitrium*.*Physcomitrella* is defined by sessile indehiscent capsules, and comprises four species, *P. patens* (Hedw.) Bruch and Schimp., *P. readeri* (Müll. Hal.) I.G. Stone and G.A.M. Scott, *P. californica* H.A. Crum and L.E. Anderson, and *P. magdalenae* De Sloover, which (Tan, 1979) treated as subspecies of *P. patens*. McDaniel et al. (2010) demonstrated that *Physcomitrella* arose from three unrelated *Physcomitrium* ancestors, and Hooper et al. (2010) described the morphological differentiation between *P. patens* and *P. readeri*. This species, which is disjunct between Australasia, eastern Asia and western North America is here consistently resolved as a sister taxon to the New Zealand endemic *Bryobeckettia*

bartlettii, which also has cleistocarpous but emergent to exserted capsules. *P. magdalenae* from central Africa may be most closely related to *P. lorentzii* from southern South America, which differs by the operculate capsules. Finally *P. patens* shares a unique common ancestor with *A. serratum*, *P. immersum* and *P. sphaericum*, which have dehiscent and except for the latter immersed capsules. The polyphyly of *Physcomitrella* is thus paralleled by that of *Physcomitrium* subg. *Cryptopyxis* (Fife, 1982), here represented by *P. immersum* and *P. lorentzii*. This subgenus differs from *Physcomitrella* most conspicuously by the operculate capsules. Indeed, the thin-walled exothecial cells, which distinguish subg. *Cryptopyxis* from other subgenera of *Physcomitrium*, are also found in *Physcomitrella*, where they compose the entire exothecium rather than being restricted to the lower half as in *Cryptopyxis*. The novel relationships proposed here may thus be congruent with patterns of variation in morphological characters previously considered of only secondary systematic importance and hence of only limited phylogenetic informativeness. The identification of diagnostic features of newly resolved lineages must await broadening the taxon sampling within the phylogenetic reconstruction to circumscribe the lineages, and will require a critical reevaluation and exploration of morphological characters for the species.

4.3. Character evolution

The current taxon sampling focuses primarily on generic exemplars and was not designed to allow for a formal reconstruction of ancestral character states. Furthermore the lack of a fully resolved and robust phylogeny, in particular for lineage III, the crown group of the Funarioideae, precludes meaningful formal reconstructions of character transformations. Among the characters used to define genera or subgenera, only the compound revoluble annulus may have arisen only once and be conserved among all descendants, composing the genus *Funaria*. The polyphyletic nature of *Entosthodon*, *Physcomitrella* and *Physcomitrium* clearly reveals, by contrast, that their diagnostic characters are either symplesiomorphies or homoplasious. *Physcomitrella* for example is defined by immersed indehiscent capsules. Neither trait is likely ancestral to the Funariaceae, the Funarioideae or lineage III. As shown above, species of *Physcomitrella* may be most closely related to either species with inoperculate emergent capsules (i.e., *Bryobeckettia*) or taxa with operculate immersed capsules (e.g., *P. immersum*), suggesting that for these species only one of the two states (indehiscence or the short seta) may be derived and diagnostic of the species in comparison to its closest relative.

The degree of symmetry of the capsule is another homoplasious character. *Entosthodon* subg. *Plagiodus* sensu Fife (1985) is segregated from other subgenera by the strongly asymmetric capsule but included in *Entosthodon* based on the free exostome teeth. The three species sampled here, *Entosthodon muhlenbergii*, *E. serratus* and *Entosthodon (Funariella) curviseta* appear only distantly related. Strongly inclined capsules occur also in *Funaria* and hence may be symplesiomorphic for the Funarioideae, and hence be relictual in these species of *Entosthodon* rather than acquired de novo.

Peristomial architecture varies considerably across the Funariaceae. It is well developed in some but not all species of *Funaria*: although always double with exostome teeth fused at their apex, the endostome can be reduced in size, such as in *F. microstoma*. Within the sister group to *Funaria*, the peristome is either completely lacking, or incomplete or reduced, with exostome teeth remaining free (Fig. 2). Although the latter types likely derived from a well developed peristome, the corollary should not follow Dollo's law whereby the loss of a complex trait is irreversible. Zander (2006), and Spitale and Petraglia (2010) argued for the possibility of peristomes being developed in descendants of ancestors that had lost them, suggesting that only the trait and not the genetic blue-print had been previously lost. Within the Funariaceae, the current position of the peristomate *E. fascicularis* within a clade of aperistomate taxa may be another example of phyletic atavism in peristome evolution, suggesting that the occurrence of a peristome in such species may result from the reactivation of ancestral developmental genetic networks.

Considering that the diversification of lineage III took place rapidly, the time between cladogenic events may be insufficient to see an accumulation of mutations that would result in the decay of such networks and hence in the irreversibility of their silencing. Although 10 my has initially been considered the threshold beyond which genes that were not kept under selection would decay and hence could not be reactivated (Collin and Cipriani, 2003; Marshall et al., 1994), recent inferences suggest that complex traits could re-evolve after tens of millions of years and possibly even after 200 mya (Wiens, 2011). The age of the Funariales is estimated at about 174 mya (Newton et al., 2007) and hence de facto leads to a much younger origin of the Funarioideae. The radiation of lineage III would thus be too recent to have allowed for the decay or loss of genetic networks underlying the development of complex trait, making their reacquisition possible.

5. Conclusions

Phylogenetic inferences from DNA sequences have repeatedly challenged the monophyly of supraspecific taxa of bryophytes as defined by morphological characters (Cox et al., 2010; Goffinet and Buck, 2004). These studies in particular highlight the widespread inadequacy of sporophytic characters as phylogenetic markers (e.g., Goffinet et al., 2004a, 2004b), and hence the need to revise current character concepts and to explore de novo the morphological space for phylogenetically meaningful traits. Sporophytic characters, and in particular peristome architecture, have been central to the classification of mosses (Crosby, 1980; Vitt, 1984; Walther, 1983) on the implicit assumption that given the critical role of peristomes in spore dispersal their architecture must be under intense selection pressure and hence be conserved (e.g., Allen et al., 1985). In the light of the phylogenetic hypotheses, it appears as if the selective pressures (or their relaxation) are in fact driving the diversification rather than the conservation of sporophytic architecture.

Phylogenetic inferences from ten loci from all genomic compartments (1) confirm the initial divergence between the Funarioideae and Pyramiduloideae, (2) support a diagnosis of *Funaria* versus *Entosthodon* based on the compound annulus and (3) reveal the polyphyly of *Entosthodon*, *Physcomitrella* and *Physcomitrium*, and thereby the homoplasy of the sporophytic characters than define these genera. This study confirms the pattern emerging from various phylogenetic study regarding the phylogenetic stability and significance of sporophytic characters in the evolutionary history of mosses. The ambiguity of the relationships of the core Funarioideae likely reflects a rapid diversification and precludes reconstructing the sequence and polarity of morphological character transformations, and thus testing of a central hypothesis, namely that character loss is irreversible. We currently seek to resolve the phylogeny of this rapid diversification through nearly exhaustive taxon sampling, especially based on extensive character sampling (Jian et al., 2008; Wortley et al., 2005) and thereby provide the necessary phylogenetic framework to address patterns, and ultimately processes in the evolution of the moss sporophyte.

Acknowledgments

Grant (DEB-0919284) from the National Science Foundation to BG funded lab work, the postdoctoral position for LY and graduate

assistantship for JMB. The authors thank Juan Carlos Villarreal A. and Wei Wang for discussion on an earlier draft of the manuscript, Paul O. Lewis for help with the SOWH test and BI methods, and Daniel Fan for performing the SS analyses. The UConn Bioinformatics Facility provided computing resources for the Bayesian and maximum likelihood analyses performed for this study. We thank the herbaria and the following colleagues for sharing material with us: Drs. Brugués, Fife, Jolley, Lüth, McDaniel, Milne, Ros, and Werner.

Appendix A. Supplementary material

Supplementary data associated with this article can be found, in the online version, at doi:10.1016/j.ympev.2011.09.010.

References

Akaike, H., 2002. A new look at the statistical model identification. IEEE Transactions on Automatic Control 19, 716–723.
Allen, B.H., Crosby, M.R., Magill, R.E., 1985. A review of the genus *Stenodictyon* (Musci). Lindbergia 11, 149–156.
Bateman, R.M., Crane, P.R., DiMichele, W.A., Kenrick, P.R., Rowe, N.P., Speck, T., Stein, W.E., 1998. Early evolution of land plants: phylogeny, physiology, and ecology of the primary terrestrial radiation. Annual Review of Ecology and Systematics 29, 263–292.
Bauer, L., Brosig, M., 1959. Zur Kenntnis reziproker Kreuzungen von Funariaceen: 1. Die Bastarde *Funaria hygrometrica* × *Physcomitrium acuminatum* und reziprok. Zeitschrift für Vererbungeslehre 90, 400–408.
Bell, N.E., Hyvönen, J., 2010. A phylogenetic circumscription of *Polytrichastrum* (Polytrichaceae): reassessment of sporophyte morphology supports molecular phylogeny. American Journal of Botany 97, 566–578.
Berenbaum, M.R., Favret, C., Schuler, M.A., 1996. On defining "key innovations" in an adaptive radiation: cytochrome P450s and papilionidae. The American Naturalist 148, 139–155.
Bond, J.E., Opell, B.D., 1998. Testing adaptive radiation and key innovation hypotheses in spiders. Evolution 52, 403–414.
Brandley, M.C., Schmitz, A., Reeder, T.W., 2005. Partitioned Bayesian analyses, partition choice, and the phylogenetic relationships of scincoid lizards. Systematic Biology 54, 373–390.
Brotherus, V.F., 1903. Musci. Splachnaceae, Oedipodiceae, Disceliaceae, Funariaceae. In: Engler, A., Prantl, K. (Eds.), Die natürlichen Pflanzenfamilien. W. Engelmann, Leipzig, pp. 498–529.
Brotherus, V.F., 1924–1925. Musci. In: Engler, A., Prantl, K. (Eds.), Die natürlichen Pflanzenfamilien, second ed., vol. 10–11. W. Engelmann, Leipzig.
Brown, J.M., Lemmon, A.R., 2007. The importance of data partitioning and the utility of Bayes factors in Bayesian phylogenetics. Systematic Biology 56, 643–655.
Brown, J.M., Hedtke, S.M., Lemmon, A.R., Lemmon, E.M., 2010. When trees grow too long: investigating the causes of highly inaccurate Bayesian branch-length estimates. Systematic Biology 59, 145–161.
Brugués, M., Ruiz, E., 2010. *Entosthodon* Schwägr. and *Funaria* Hedw. In: Guerra, J., Brugués, M., Cano, M.J., Ros, R.M. (Eds.), Flora Briofítica Ibérica, vol. IV. University of Murcia, Murcia, Spain, pp. 44–62.
Bryan, V.S., 1957. Cytotaxonomic studies in the Ephemeraceae and Funariaceae. The Bryologist 60, 103–126.
Buck, W.R., Goffinet, B., Shaw, A.J., 2000. Testing morphological concepts of orders of pleurocarpous mosses (Bryophyta) using phylogenetic reconstructions based on *trnL–trnF* and *rps4* sequences. Molecular Phylogenetics and Evolution 16, 180–198.
Buckley, T.R., 2002. Model misspecification and probabilistic tests of topology: evidence from empirical data sets. Systematic Biology 51, 509–523.
Burleigh, J.G., Mathews, S., 2004. Phylogenetic signal in nucleotide data from seed plants: implications for resolving the seed plant tree of life. American Journal of Botany 91, 1599–1613.
Castoe, T.A., Doan, T.M., Parkinson, C.L., 2004. Data partitions and complex models in Bayesian analysis: the phylogeny of gymnophthalmid lizards. Systematic Biology 53, 448–469.
Caterino, M.S., Reed, R.D., Kuo, M.M., Sperling, F.A.H., 2001. A partitioned likelihood analysis of swallowtail butterfly phylogeny (Lepidoptera: Papilionidae). Systematic Biology 50, 106–127.
Collin, R., Cipriani, R., 2003. Dollo's law and the re-evolution of shell coiling. Proceedings of the Royal Society of London. Series B: Biological Sciences 270, 2551–2555.
Corley, M.F.V., Crundwell, A.C., Düll, R., Hill, M.O., Smith, A.J.E., 1981. Mosses of Europe and the Azores: an annotated list of species, with synonyms from the recent literature. Journal of Bryology 11, 609–689.
Cove, D., 2005. The moss *Physcomitrella patens*. Annual Review of Genetics 39, 339–358.
Cox, C.J., Goffinet, B., Wickett, N.J., Boles, S.B., Shaw, A.J., 2010. Moss diversity: a molecular phylogenetic analysis of genera. Phytotaxa 9, 175–195.
Crosby, M.R., 1980. The diversity and relationships of mosses. In: Taylor, R.J., Leviton, A.E. (Eds.), The Mosses of North America. Pacific Division, American Association for the Advancement of Science, San Francisco, California, USA, pp. 115–129.
Crosby, M.R., Magill, R.E., Allen, B., He, S., 1999. A Checklist of the Mosses. Missouri Botanical Garden, St. Louis.
Crum, H.A., Anderson, L.E., 1981. Mosses of Eastern North America, vol. 1 and 2. Columbia University Press, New York.
Drouin, G., Daoud, H., Xia, J., 2008. Relative rates of synonymous substitutions in the mitochondrial, chloroplast and nuclear genomes of seed plants. Molecular Phylogenetics and Evolution 49, 827–831.
Edgar, R.C., 2004. MUSCLE: multiple sequence alignment with high accuracy and high throughput. Nucleic Acids Research 32, 1792–1797.
Edwards, S., 1984. Homologies and inter-relationships of moss peristomes. In: Schuster, R.M. (Ed.), New Manual of Bryology, vol. 2. Hattori Botanical Laboratory, Nichinan, Japan, pp. 658–695.
Fan, Y., Wu, R., Chen, M.H., Kuo, L., Lewis, P.O., 2010. Choosing among partition models in Bayesian phylogenetics. Molecular Biology and Evolution 28, 523–532.
Felsenstein, J., 1985. Confidence limits on phylogenies: an approach using the bootstrap. Evolution 39, 783–791.
Fife, A.J., 1982. A Generic Revision of the Funariaceae (Bryophyta: Musci). Ph.D. Dissertation, University of Michigan, Ann Arbor.
Fife, A.J., 1985. A generic revision of the Funariaceae (Bryophyta: Musci). Part I. Journal of the Hattori Botanical Laboratory 58, 149–196.
Frahm, J.P., 1995. Laubmoose. In: Frey, W., Frahm, J.P., Fischer, E., Lobin, W. (Eds.), Die Moos-und Farnpflanzen Europas. Gustav Fisher Verlag, Stuttgart, pp. 121–318.
Freeman, P.W., 2000. Macroevolution in Microchiroptera: recoupling morphology and ecology with phylogeny. Evolutionary Ecology Research 2, 317–335.
Goffinet, B., Buck, W.R., 2004. Systematics of the Bryophyta (mosses): from molecules to a revised classification. Monographs in Systematic Botany from the Missouri Botanical Garden 98, 205–239.
Goffinet, B., Cox, C.J., 2000. Phylogenetic relationships among basal-most arthrodontous mosses with special emphasis on the evolutionary significance of the Funariineae. Bryologist 103, 212–223.
Goffinet, B., Shaw, A.J., 2002. Independent origins of cleistocarpy in the Splachnaceae: analyses of cpDNA sequences and polyphyly of the Voitioideae (Bryophyta). Systematic Botany 27, 203–208.
Goffinet, B., Shaw, J., Anderson, L.E., Mishler, B.D., 1999. Peristome development in mosses in relation to systematics and evolution. V. Diplolepideae: Orthotrichaceae. The Bryologist 102, 581–594.
Goffinet, B., Cox, C.J., Shaw, A.J., Hedderson, T.A.J., 2001. The Bryophyta (Mosses): systematic and evolutionary inferences from an *rps4* gene (cpDNA) phylogeny. Annals of Botany 87, 191–208.
Goffinet, B., Shaw, A.J., Cox, C.J., 2004a. Phylogenetic inferences in the dung-moss family Splachnaceae from analyses of cpDNA sequence data and implications for the evolution of entomophily. American Journal of Botany 91, 748–759.
Goffinet, B., Shaw, A.J., Cox, C.J., Wickett, N.J., Boles, S.B., 2004b. Phylogenetic inferences in the Orthotrichoideae (Orthotrichaceae, Bryophyta) based on variation in four loci from all genomes. Monographs in Systematic Botany from the Missouri Botanical Garden 98, 270–289.
Goffinet, B., Wickett, N.J., Werner, O., Ros, R.M., Shaw, A.J., Cox, C.J., 2007. Distribution and phylogenetic significance of the 71-kb inversion in the plastid genome in Funariidae (Bryophyta). Annals of Botany 99, 747–753.
Goffinet, B., Buck, W.R., Shaw, A.J., 2009. Morphology, anatomy, and classification of the Bryophyta. In: Goffinet, B., Shaw, A.J. (Eds.), Bryophyte Biology, second ed. Cambridge University Press, Cambridge, UK, pp. 55–138.
Goffinet, B., Budke, J.M., Newman, L.C., in press. Micromitriaceae: a new family of reduced mosses displaying a neotenous plant body in both generations. Taxon..
Goldman, N., Anderson, J.P., Rodrigo, A.G., 2000. Likelihood-based tests of topologies in phylogenetics. Systematic biology 49, 652–670.
Hedderson, T.A., Cox, C.J., Gibbings, J.G., 1999. Phylogenetic relationships of the Wardiaceae (Musci); evidence from 18s rRNA and rps4 gene sequences. Bryologist 102, 26–31.
Holyoak, D.T., Pedersen, N., 2007. Conflicting molecular and morphological evidence of evolution within the Bryaceae (Bryopsida) and its implications for generic taxonomy. Journal of Bryology 29, 111–124.
Hooper, E.J., Duckett, J.G., Cuming, A.C., Kunin, W.E., Pressel, S., 2010. *Ephemerella readeri* Müll. Hal. (*Physcomitrella readeri* (Müll. Hal.) I.G. Stone, G.A.M. Scott, Funariidae, Bryophyta): a genus and species new to Europe. Journal of Bryology 32, 256–264.
Hughes, C., Eastwood, R., 2006. Island radiation on a continental scale: exceptional rates of plant diversification after uplift of the Andes. PNAS 103, 10334–10339.
Huson, D.H., Bryant, D., 2006. Application of phylogenetic networks in evolutionary studies. Molecular Biology and Evolution 23, 254–267.
Huson, D.H., Dezulian, T., Klopper, T., Steel, M.A., 2004. Phylogenetic super-networks from partial trees. IEEE/ACM Transactions on Computational Biology and Bioinformatics (TCBB) 1, 151–158.
Jian, S., Soltis, P.S., Gitzendanner, M.A., Moore, M.J., Li, R., Hendry, T.A., Qiu, Y.L., Dhingra, A., Bell, C.D., Soltis, D.E., 2008. Resolving an ancient, rapid radiation in Saxifragales. Systematic Biology 57, 38–57.
Kass, R.E., Raftery, A.E., 1995. Bayes factors. Journal of the American Statistical Association 90, 773–795.

Kishino, H., Hasegawa, M., 1989. Evaluation of the maximum likelihood estimate of the evolutionary tree topologies from DNA sequence data, and the branching order in Hominoidea. Journal of Molecular Evolution 29, 170–179.
Knight, C., Perroud, P.F., Cove, D., 2009. The Moss *Physcomitrella patens*. Wiley-Blackwell.
Koch, M.A., Dobeš, C., Kiefer, C., Schmickl, R., Klimeš, L., Lysak, M.A., 2007. Supernetwork identifies multiple events of plastid *trn*F (GAA) pseudogene evolution in the Brassicaceae. Molecular Biology and Evolution 24, 63–73.
Lemey, P., Salemi, M., Vandamme, A.M., 2009. The Phylogenetic Handbook: A Practical Approach to Phylogenetic Analysis and Hypothesis Testing, second ed. Cambridge University Press, Cambridge.
Lewis, P.O., Holder, M.T., Swofford, D.L., 2008. Phycas: Software for Phylogenetic Analysis. <http://www.phycas.org/>.
Li, C., Lu, G., Ortí, G., 2008. Optimal data partitioning and a test case for ray-finned fishes (Actinopterygii) based on ten nuclear loci. Systematic Biology 57, 519–539.
Lindberg, S.O., 1870. *Manipulus muscorum primus*. F. Fl. Fenn. 11, 42–72.
Lindberg, S.O., 1879. Musci Scandinavici in systemate novo naturali dispositi. Officina Iesaiae, Upsala.
Maddison, W.P., Maddison, D.R., 2010. Mesquite: A Modular System for Evolutionary Analysis. Version 2.74, <http://mesquiteproject.org>.
Marshall, D.C., 2010. Cryptic failure of partitioned Bayesian phylogenetic analyses: lost in the land of long trees. Systematic Biology 59, 108–117.
Marshall, C.R., Raff, E.C., Raff, R.A., 1994. Dollo's law and the death and resurrection of genes. PNAS 91, 12283–12287.
Mason-Gamer, R.J., Kellogg, E.A., 1996. Testing for phylogenetic conflict among molecular data sets in the tribe Triticeae (Gramineae). Systematic Biology 45, 524–545.
McCune, A.R., 1997. How fast is speciation? Molecular, geological, and phylogenetic evidence from adaptive radiations of fishes. In: Givnish, T.J., Sytsma, K.J. (Eds.), Molecular Evolution and Adaptive Radiation. Cambridge University Press, Cambridge, pp. 585–610.
McDaniel, S.F., Von Stackelberg, M., Richardt, S., Quatrano, R.S., Reski, R., Rensing, S.A., 2010. The speciation history of the *Physcomitrium–Physcomitrella* species complex. Evolution 64, 217–231.
McGuire, J.A., Witt, C.C., Altshuler, D.L., Remsen, J.V., 2007. Phylogenetic systematics and biogeography of hummingbirds: Bayesian and maximum likelihood analyses of partitioned data and selection of an appropriate partitioning strategy. Systematic Biology 56, 837–856.
McIntosh, T.T., 2007. Funariaceae Schwägrichen. In: Flora of North America Editorial Committee (Ed.), Flora of North America. Bryophytes: Mosses, Part 1, vol. 27. Oxford University Press, New York, pp. 180–199.
Miller, D.H., Miller, H.A., 2007. *Entosthodon* and *Funaria*. In: Flora of North America Editorial Committee (Ed.), Flora of North America North of Mexico. Bryophytes: Mosses, Part 1, vol. 27. Oxford University Press, New York, pp. 182–194.
Mower, J.P., Touzet, P., Gummow, J.S., Delph, L.F., Palmer, J.D., 2007. Extensive variation in synonymous substitution rates in mitochondrial genes of seed plants. BMC Evolutionary Biology 7, 135.
Mueller, C., 1849–1851. Synopsis muscorum frodorosum omnium hucusque cognitorum, vol. 1 and 2. A. Foerstner, Berlin.
Natcheva, R., Cronberg, N., 2004. What do we know about hybridization among bryophytes in nature? Canadian Journal of Botany 82, 1687–1704.
Newton, A.E., Wikstrom, N., Bell, N., Forrest, L., Ignatov, M., Tangney, R.S., 2007. Dating the diversification of the pleurocarpous mosses. In: Newton, A.E., Tangney, R.S. (Eds.), Pleurocarpous Mosses: Systematics and Evolution. CRC Press, Boca Raton, pp. 337–366.
Nicholson, W.E., 1931. Hybridity among the bryophytes. Revue Bryologique 4, 138–140.
Nylander, J., 2004. MrModeltest v2. Program Distributed by the Author. Evolutionary Biology Centre, Uppsala University.
Nylander, J.A.A., Ronquist, F., Huelsenbeck, J.P., Nieves-Aldrey, J., 2004. Bayesian phylogenetic analysis of combined data. Systematic Biology 53, 47–67.
Ochyra, R., 1983. The rediscovery of *Loiseaubryum ephermeroides* Bizot (Musci: Funariaceae) in Nigeria. Acta Botanica Hungarica 29, 173–179.
Paton, J.A., Pearce, J.V., 1957. The occurrence, structure and functions of the stomata in British bryophytes. Transactions of the British Bryological Society 3, 228–259.
Pettet, A., 1964. Hybrid sporophytes in the Funariaceae. Transactions of the British Bryological Society 4, 642–648.
Posada, D., 2008. JModelTest: phylogenetic model averaging. Molecular Biology and Evolution 25, 1253–1256.
Pupko, T., Huchon, D., Cao, Y., Okada, N., Hasegawa, M., 2002. Combining multiple data sets in a likelihood analysis: which models are the best? Molecular Biology and Evolution 19, 2294–2307.
Rambaut, A., Drummond, A.J., 2009. Tracer v1. 5. <http://tree.bio.ed.ac.uk/software/tracer/>.
Rambaut, A., Grassly, N.C., 1997. Seq-Gen: an application for the Monte Carlo simulation of DNA sequence evolution along phylogenetic trees. Computer Applications in the Biosciences 13, 235–238.
Rensing, S.A. et al., 2008. The *Physcomitrella* genome reveals evolutionary insights into the conquest of land by plants. Science 319, 64–69.
Ronquist, F., Huelsenbeck, J., 2003. MrBayes 3: Bayesian phylogenetic inference under mixed models. Bioinformatics 19, 1572–1574.
Schaefer, D.G., Zrÿd, J.P., 2001. The moss *Physcomitrella patens*, now and then. Plant Physiology 127, 1430–1438.
Schluter, D., 2000. The Ecology of Adaptive Radiation. Oxford University Press, Oxford.
Schmidt, H., Strimmer, K., Vingron, M., Von Haeseler, A., 2002. TREE-PUZZLE: maximum likelihood phylogenetic analysis using quartets and parallel computing. Bioinformatics 18, 502–504.
Schwartz, O.M., 1994. The development of the peristome-forming layers in the Funariaceae. International Journal of Plant Sciences 155, 640–657.
Sérgio, C., 1988. Morphological, karyological and phytogeographic observations on *Entosthodon curvisetus* (Schwager.) C. Müll. as a basis for a new genus, *Funariella* Sérgio (Funariaceae: Musci). Orsis 3, 5–13.
Shaw, J., Anderson, L.E., Mishler, B.D., 1989. Peristome development in mosses in relation to systematics and evolution. III. *Funaria hygrometrica*, *Bryum pseudocapillare*, and *B. bicolor*. Systematic Botany 14, 24–36.
Shaw, A.J., Cox, C.J., Goffinet, B., Buck, W.R., Boles, S.B., 2003. Phylogenetic evidence of a rapid radiation of pleurocarpous mosses (Bryophyta). Evolution 57, 2226–2241.
Shimodaira, H., 2002. An approximately unbiased test of phylogenetic tree selection. Systematic Biology 51, 492–508.
Shimodaira, H., Hasegawa, M., 1999. Multiple comparisons of log-likelihoods with applications to phylogenetic inference. Molecular Biology and Evolution 16, 1114–1116.
Shimodaira, H., Hasegawa, M., 2001. CONSEL: for assessing the confidence of phylogenetic tree selection. Bioinformatics 17, 1246–1247.
Smith, A.J.E., 1978. The Moss Flora of Britain and Ireland. Cambridge University Press, Cambridge.
Smith, A.J.E., 2004. The Moss Flora of Britain and Ireland. Cambridge University Press, Cambridge, UK.
Soltis, D.E., Soltis, P.S., Endress, P.K., Chase, M.W., 2005. Phylogeny and Evolution of Angiosperms. Sinauer Associates, Sunderland, Massachusetts.
Spitale, D., Petraglia, A., 2010. *Palustriella falcata* (Brid.) Hedenäs (Amblystegiaceae, Bryopsida) with pluristratose lamina: morphological variability of specimens in springs of the Italian Alps. Plant Systematics and Evolution 286, 59–68.
Stamatakis, A., 2006. RAxML-VI-HPC: maximum likelihood-based phylogenetic analyses with thousands of taxa and mixed models. Bioinformatics 22, 2688–2690.
Stech, M., Quandt, D., 2010. 20,000 species and five key markers: the status of molecular bryophyte phylogenetics. Phytotaxa 9, 196–228.
Strimmer, K., Rambaut, A., 2002. Inferring confidence sets of possibly misspecified gene trees. Proceedings of the Royal Society of London. Series B: Biological Sciences 269, 137–142.
Strimmer, K., Von Haeseler, A., 1997. Likelihood-mapping: a simple method to visualize phylogenetic content of a sequence alignment. Proceedings of the National Academy of Sciences of the United States of America 94, 6815–6819.
Sugiura, C., Kobayashi, Y., Aoki, S., Sugita, C., Sugita, M., 2003. Complete chloroplast DNA sequence of the moss *Physcomitrella patens*: evidence for the loss and relocation of *rpo*A from the chloroplast to the nucleus. Nucleic Acids Research 31, 5324–5331.
Swofford, D., 2003. PAUP*: Phylogenetic Analysis Using Parsimony (*and Other Methods), Version 4.0 b10. Sinauer Associates, Sunderland, MA.
Talavera, G., Castresana, J., 2007. Improvement of phylogenies after removing divergent and ambiguously aligned blocks from protein sequence alignments. Systematic Biology 56, 564–577.
Tamura, K., Dudley, J., Nei, M., Kumar, S., 2007. MEGA4: molecular evolutionary genetics analysis (MEGA) software version 4.0. Molecular Biology and Evolution 24, 1596–1599.
Tan, B.C., 1979. A new classification for the genus *Physcomitrella* B.S.G. Journal of the Hattori Botanical Laboratory 46, 327–336.
Terasawa, K., Odahara, M., Kabeya, Y., Kikugawa, T., Sekine, Y., Fujiwara, M., Sato, N., 2007. The mitochondrial genome of the moss *Physcomitrella patens* sheds new light on mitochondrial evolution in land plants. Molecular Biology and Evolution 24, 699–709.
Vamosi, J.C., Vamosi, S.M., 2011. Factors influencing diversification in angiosperms: at the crossroads of intrinsic and extrinsic traits. American Journal of Botany 98, 460–471.
Verheyen, E., Salzburger, W., Snoeks, J., Meyer, A., 2003. Origin of the superflock of cichlid fishes from Lake Victoria, East Africa. Science 300, 325–329.
Vitt, D.H., 1981. Adaptive modes of the moss sporophyte. The Bryologist 84, 166–186.
Vitt, D.H., 1982. Bryopsida. In: Parker, S.P. (Ed.), Synopsis and Classification of Living Organisms. McGraw-Hill, New York, pp. 307–336.
Vitt, D.H., 1984. Classification of the Bryopsida. In: Schuster, R.M. (Ed.), New Manual of Bryology, vol. 2. Hattori Botanical Laboratory, Nichinan, Japan, pp. 696–759.
Vitt, D.H., 2000. The classification of mosses: two-hundred years after Hedwig. Nova Hedwigia 70, 25–36.
von Wettstein, F., 1924. Morphologie und Physiologie des Formwechsels der Moose auf genetischer Grundlage. I. Zeitschrift Abstammungs-und Vererbungeslehre 33, 1–236.
von Wettstein, F., 1932. Genetik. In: Verdoorn, F. (Ed.), Manual of Bryology. Martinus Nijhoff, The Hague, Netherlands, pp. 233–272.
Walther, K., 1983. Bryophytina. Laubmoose. In: Gerloff, J., Poelt, J. (Eds.), A. Engler's Syllabus der pflanzenfamilien, vol. 2. Bornträger, Berlin, pp. 1–108.
Ward, P.S., Brady, S.G., Fisher, B.L., Schultz, T.R., 2010. Phylogeny and biogeography of dolichoderine ants: effects of data partitioning and relict taxa on historical inference. Systematic Biology 59, 342–362.
Werner, O., Ros, R.M., Goffinet, B., 2007. A reconsideration of the systematic position of *Goniomitrium* (Funariaceae) based on chloroplast sequence markers. The Bryologist 110, 108–114.

Wheeler, J.A., 2000. Molecular phylogenetic reconstructions of the marchantioid liverwort radiation. Bryologist 103, 314–333.
Whitfield, J.B., Kjer, K.M., 2008. Ancient rapid radiations of insects: challenges for phylogenetic analysis. Annual Review of Entomology 53, 449–472.
Whitfield, J.B., Lockhart, P.J., 2007. Deciphering ancient rapid radiations. Trends in Ecology and Evolution 22, 258–265.
Wiens, J.J., 2011. Re-evolution of lost mandibular teeth in frogs after more than 200 million years, and re-evaluating Dollo's law. Evolution 65, 1283–1296.
Wortley, A.H., Rudall, P.J., Harris, D.J., Scotland, R.W., 2005. How much data are needed to resolve a difficult phylogeny? Case study in Lamiales. Systematic Biology 54, 697–709.
Zander, R., 2006. The *Pottiaceae* s. str. as an evolutionary Lazarus taxon. Journal of the Hattori Botanical Laboratory 100, 581–602.
Zwickl, D.J., 2006. Genetic Algorithm Approaches for the Phylogenetic Analysis of Large Biological Sequence Datasets under the Maximum Likelihood Criterion. Ph.D. dissertation, The University of Texas at Austin.